

Asymptotics of Some Nonlinear Eigenvalue Problems Modelling a MEMS Capacitor: Part II: Multiple Solutions and Singular Asymptotics

A. E. LINDSAY and M. J. WARD

Department of Mathematics, University of British Columbia, Vancouver, British Columbia, V6T 1Z2, Canada,

(Received April 17th, 2010)

Some nonlinear eigenvalue problems related to the modelling of the steady-state deflection of an elastic membrane associated with a MEMS capacitor under a constant applied voltage are analyzed using formal asymptotic methods. These problems consist of certain singular perturbations of the basic membrane nonlinear eigenvalue problem $\Delta u = \lambda/(1+u)^2$ in Ω with $u = 0$ on $\partial\Omega$, where Ω is the unit ball in \mathbb{R}^2 . It is well-known that the radially symmetric solution branch to this basic membrane problem has an infinite fold-point structure with $\lambda \rightarrow 4/9$ as $\varepsilon \equiv 1 - \|u\|_\infty \rightarrow 0^+$. One focus of this paper is to develop a novel singular perturbation method to analytically determine the limiting asymptotic behaviour of this infinite fold-point structure in terms of two constants that must be computed numerically. This theory is then extended to certain generalizations of the basic membrane problem in the N -dimensional unit ball. The second main focus of this paper is to analyze the effect of two distinct perturbations of the basic membrane problem in the unit disk resulting from including either a bending energy term of the form $-\delta\Delta^2 u$ to the operator, or inserting a concentric inner undeflected disk of radius δ . For each of these perturbed problems, it is shown numerically that the infinite fold-point structure for the basic membrane problem is destroyed when $\delta > 0$, and that there is a maximal solution branch for which $\lambda \rightarrow 0$ as $\varepsilon \equiv 1 - \|u\|_\infty \rightarrow 0^+$. For $\delta > 0$, a novel singular perturbation analysis is used in the limit $\varepsilon \rightarrow 0^+$ to construct the limiting asymptotic behaviour of the maximal solution branch for the biharmonic problem in the unit slab and the unit disk, and for the annulus problem in the unit disk. The asymptotic results for the bifurcation curves are shown to compare very favourably with full numerical results.

Key words: Biharmonic nonlinear eigenvalue problem, Matched asymptotic expansions, Infinite fold-point structure, Logarithmic switchback terms.

1 Introduction

Micro-Electromechanical Systems (MEMS) combine electronics with micro-size mechanical devices to design various types of microscopic machinery (cf. [22]). A key component of many MEMS systems is the simple MEMS capacitor shown in Fig. 1. The upper part of this device consists of a thin deformable elastic plate that is held clamped along its boundary, and which lies above a fixed ground plate. When a voltage V is applied to the upper plate, the upper plate can exhibit a significant deflection towards the lower ground plate.

By including the effect of a bending energy, it was shown in [22] that the dimensionless steady state deflection $u(x)$ of the upper plate satisfies the fourth-order nonlinear eigenvalue problem

$$-\delta\Delta^2 u + \Delta u = \frac{\lambda}{(1+u)^2}, \quad x \in \Omega; \quad u = \partial_n u = 0 \quad x \in \partial\Omega. \quad (1.1)$$

Here, the positive constant δ represents the relative effects of tension and rigidity on the deflecting plate, and $\lambda \geq 0$ represents the ratio of electric forces to elastic forces in the system, and is directly proportional to the square of the voltage V applied to the upper plate. The boundary conditions in (1.1) assume that the upper plate is in a clamped state along the rim of the plate. The model (1.1) was derived in [22] from a narrow-gap asymptotic analysis.

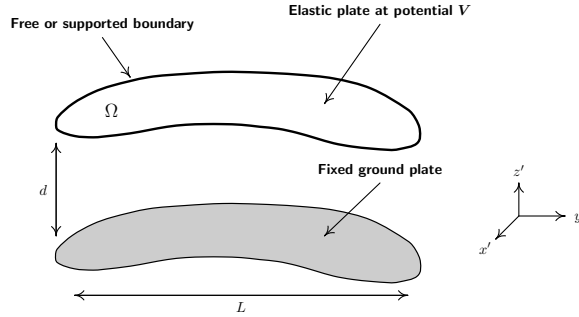


FIGURE 1. Schematic plot of the MEMS capacitor with a deformable elastic upper surface that deflects towards the fixed lower surface under an applied voltage.

A special limiting case of (1.1) is when $\delta = 0$, so that the upper surface is modeled by a membrane rather than by a plate. Omitting the requirement that $\partial_n u = 0$ on $\partial\Omega$, (1.1) reduces to the basic MEMS membrane problem

$$\Delta u = \frac{\lambda}{(1+u)^2}, \quad x \in \Omega; \quad u = 0 \quad x \in \partial\Omega. \quad (1.2)$$

In the unit disk, this simple nonlinear eigenvalue problem has been studied from a dynamical systems viewpoint in [16], [23], and [10]. For the unit disk in \mathbb{R}^2 , one of the key qualitative features for (1.2) is that the bifurcation diagram of $\|u\|_\infty$ versus λ for radially symmetric solutions of (1.2) has an infinite number of fold points with $\lambda \rightarrow 4/9$ as $\|u\|_\infty \rightarrow 1^-$ (cf. [16], [23], [10]). Rigorous analytical bounds for the pull-in voltage instability threshold, representing the fold point location λ_c at the end of the minimal solution branch for (1.2), have also been derived (cf. [23], [10], [8]). For the unit disk, a plot of the numerically computed bifurcation diagram showing the beginning of the infinite fold-point structure is shown in Fig. 2.

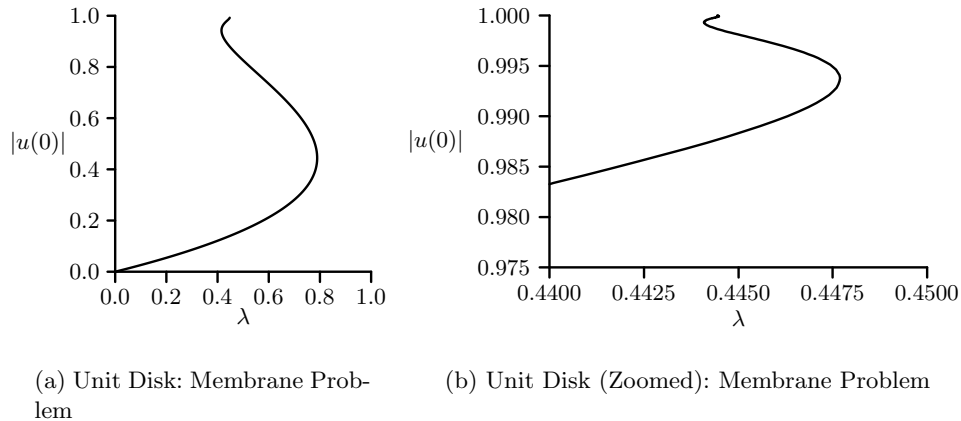


FIGURE 2. Numerical solutions for $|u(0)|$ versus λ computed from (1.2) for the unit disk $\Omega \equiv \{|x| \leq 1\}$ in \mathbb{R}^2 . The magnified figure on the right shows the beginning of the infinite set of fold points.

In Fig. 3 the numerically computed bifurcation diagram of $|u(0)|$ versus λ for the biharmonic problem (1.1) is plotted for several geometries and for various values of $\delta > 0$. These numerical results, computed by using either the shooting or pseudo-arclength continuation methods of [21], indicate that the presence of the biharmonic term $-\delta\Delta^2 u$ in (1.1) destroys the infinite fold-point structure associated with the membrane problem (1.2) in the unit

disk and unit square geometries. Moreover, these numerical results suggest that there is a maximal solution branch with the limiting behaviour $\lambda \rightarrow 0$ as $\|u\|_\infty \rightarrow 1^-$.

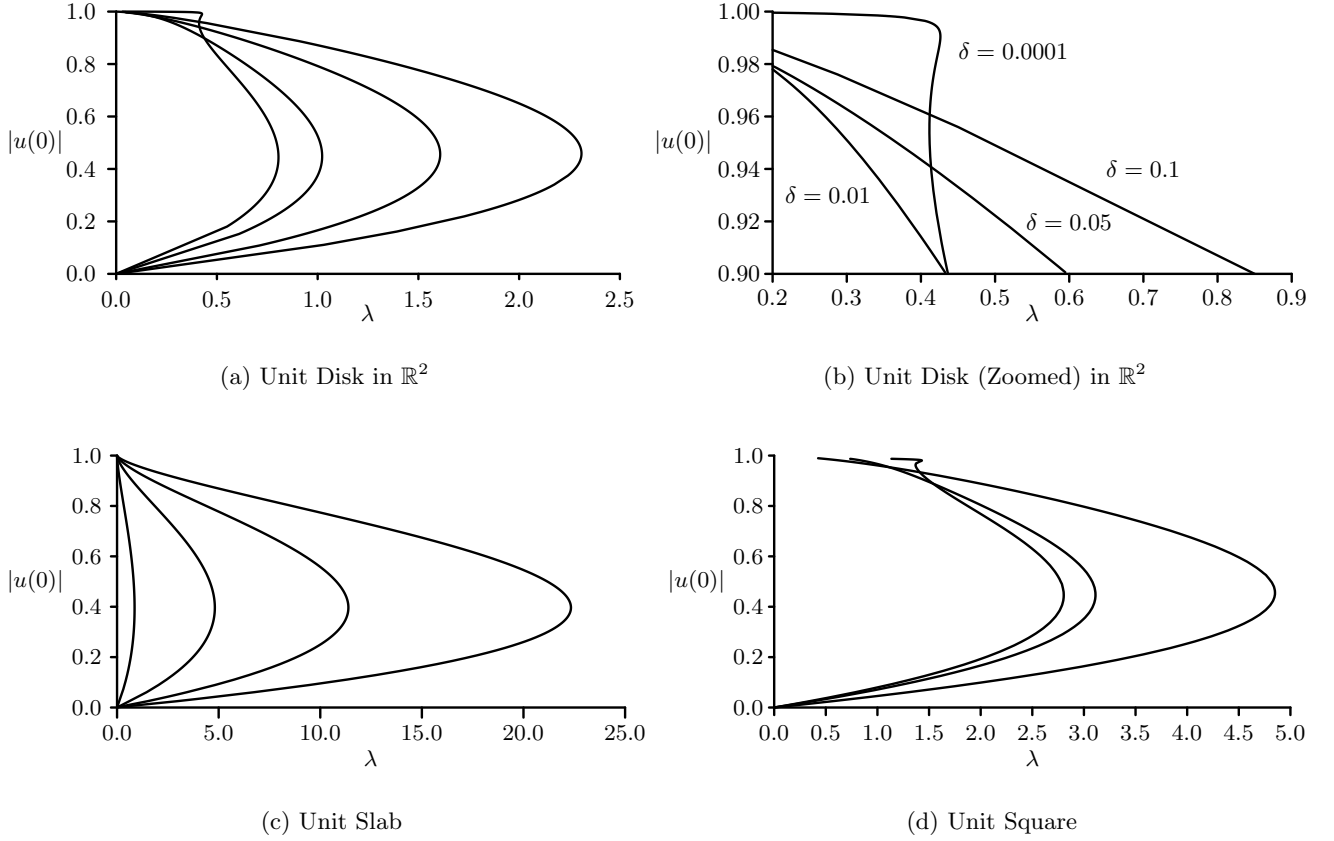


FIGURE 3. Top Left: Numerical solution branches of (1.1) for the unit disk in \mathbb{R}^2 . From left to right the curves correspond to $\delta = 0.0001, 0.01, 0.05, 0.1$. Top Right: A magnified portion of the top left figure. Bottom Left: Numerical solution branches of (1.1) for the slab $|x| \leq 1/2$. From left to right the curves correspond to $\delta = 0.1, 1.0, 2.5, 5.0$. Bottom Right: Numerical solution branches for the unit square $-1/2 \leq x_1, x_2 \leq 1/2$, where $|u(0)|$ denotes the value at the centre of the square. From left to right the curves correspond to $\delta = 0.0001, 0.001, 0.01$.

From a mathematical viewpoint, a generalization of (1.2) that has received some theoretical attention is the following problem with the variable coefficient $|x|^\alpha$ in an N -dimensional domain Ω :

$$\Delta u = \frac{\lambda |x|^\alpha}{(1+u)^2}, \quad x \in \Omega; \quad u = 0 \quad x \in \partial\Omega. \quad (1.3)$$

In \mathbb{R}^2 this problem models the steady-state membrane deflection with a variable permittivity profile in the membrane (see [23]). For the unit ball in \mathbb{R}^N , and for $\alpha = 0$, the range of N for which an infinite fold-point structure exists was established in [16] by using a rigorous dynamical systems approach. Similar results, but for the case $\alpha > 0$ and for other non-power-law coefficients, were obtained in [12], [11], [8], and [5], by using a PDE-based approach. Upper and lower bounds for the pull-in voltage threshold λ_c , representing the saddle-node bifurcation point along the minimal solution branch, have been derived and the regularity properties of the extremal solution at the end of the minimal solution branch have been studied (cf. [8] and [5]). With regards to domains of other shape, in [13] it was proved that there are an infinite number of fold points for (1.2) in a certain class of symmetric domains in \mathbb{R}^2 .

For star-shaped domains in dimension $N \geq 3$ it was proved in [4] that (1.3) has a unique solution for λ sufficiently small.

The first main goal in this paper is to introduce a systematic method, based on the method of matched asymptotic expansions, to formally construct the limiting asymptotic behaviour as $\varepsilon \equiv 1 - \|u\|_\infty \rightarrow 0^+$ of the radially symmetric solution branches for (1.3) in the unit ball in N dimensions. In contrast to the rigorous, but more qualitative approaches of [16], [12], and [5], our formal asymptotic approach provides an *explicit* analytical characterization of the infinite fold-point structure for (1.3) in terms of two constants, depending on α and N , which must be computed numerically from an ODE initial value problem. In the limit $\varepsilon \rightarrow 0$, a boundary layer is required near the centre of the disk in order to resolve the nearly singular nonlinearity in (1.3) near the origin. By matching the far-field behaviour of this boundary layer solution to a certain singular outer solution, and by using a solvability condition, an explicit characterization of the infinite fold-point structure is obtained. For the range of parameters α and N where an infinite fold-point structure exists for (1.3) exists in the unit ball, our explicit asymptotic results for the bifurcation curve are found to agree very well with the corresponding full numerical result even when ε is not too small.

In contrast to (1.2) and (1.3), there are only a few rigorous results available for the biharmonic problem (1.1) under clamped boundary conditions $u = \partial_n u = 0$ on $\partial\Omega$. In [2], the regularity of the minimal solution branch, together with bounds for the pull-in voltage, was established for the pure biharmonic problem $-\Delta^2 u = \lambda/(1+u)^2$ in the N -dimensional unit ball. Related results for the regularity properties of the extremal solution for the pure biharmonic problem were obtained in [1]. By using a formal asymptotic approach, in [21] perturbation results for the pull-in voltage threshold were obtained for (1.1) for the limiting cases $\delta \ll 1$ and for $\delta \gg 1$ in the unit disk in \mathbb{R}^2 and in the slab. However, as yet, there has been no precise analytical description of the maximal solution branch to (1.1) for clamped boundary conditions. We remark that for the simpler case of Navier boundary conditions $u = \Delta u = 0$ on $\partial\Omega$ there are some results regarding regularity of the maximal solution branch and solution multiplicity for various dimensions N (see [15], [14], and [20]). Precise rigorous results for (1.3) and (1.1) are surveyed in [6].

The second main goal in this paper is to develop a formal asymptotic method, based on the method of matched asymptotic expansions, to provide an *explicit* analytical characterization of the asymptotic behaviour of the maximal solution branch to (1.1) in the limit $\varepsilon = 1 - \|u\|_\infty \rightarrow 0^+$ for which $\lambda \rightarrow 0$. This problem is studied for the unit slab and for the unit disk in \mathbb{R}^2 . For these domains, explicit asymptotic expansions for λ as $\varepsilon \rightarrow 0$ are derived for any $\delta > 0$, and the results are shown to compare very favourably with full numerical results. The solution u to (1.1) in the limit $\varepsilon \rightarrow 0$ has a strong concentration near the origin owing to the nearly singular behaviour of the nonlinearity in (1.1). The singular perturbation analysis required to resolve this region of concentration and match to an outer solution relies heavily on the systematic use of logarithmic switchback terms. Such terms are notorious in the asymptotic analysis of some PDE models of low Reynolds number flows (cf. [18], [19], [26], [27]).

Another modification of the basic membrane problem (1.2) in the unit disk in \mathbb{R}^2 , which also destroys the infinite fold-point structure for (1.2), is to pin the rim of a concentric inner disk in an undeflected state (cf. [24]). The perturbed problem in the concentric annular domain $0 < \delta < |x| < 1$ in \mathbb{R}^2 is

$$\Delta u = \frac{\lambda}{(1+u)^2}, \quad 0 < \delta < r < 1; \quad u = 0 \quad \text{on} \quad |x| = 1 \quad \text{and} \quad |x| = \delta. \quad (1.4)$$

The introduction of a clamped inner disk has three main effects. It increases the pull-in voltage rather significantly

(cf. [21]), it destroys the infinite fold-point structure associated with (1.2), and it allows for the existence of non-radially symmetric solutions that bifurcate off of the secondary radially symmetric solution branch (cf. [24], [7]).

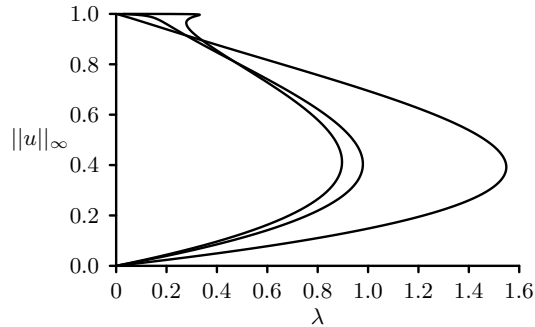


FIGURE 4. Numerical solutions for $\|u\|_\infty$ versus λ computed from the annulus problem (1.4) in the annulus $\delta < r < 1$. From left to right the curves correspond to $\delta = 0.00001, 0.001, 0.1$.

For various values of δ , a numerically computed bifurcation diagram for (1.4) obtained by using the numerical approach of [21] is shown in Fig. 4. For $\delta > 0$, this plot shows that the effect of the perturbation is to destroy the infinite fold-point structure associated with the membrane problem (1.2), and it suggests the existence of a maximal solution branch for which $\lambda \rightarrow 0$ as $\varepsilon \equiv 1 - \|u\|_\infty \rightarrow 0^+$. For a fixed $\delta > 0$, we use the method of matched asymptotic expansions to calculate the limiting asymptotic behaviour of the maximal solution branch for (1.4) in the unit disk.

From a mathematical viewpoint, the problems (1.1) and (1.4) are singular perturbations of (1.2) in that they destroy the infinite fold-point structure for the basic membrane problem (1.2) in \mathbb{R}^2 . Our formal asymptotic approach, based on introducing a small parameter $\varepsilon \equiv 1 - \|u\|_\infty \ll 1$, leads to a nonlinearity that is nearly singular in a small region of concentration inside the domain. By resolving this localized region of concentration using the method of matched asymptotic expansions, explicit characterizations of the limiting asymptotic behaviour of the maximal solution branch for (1.1) and (1.4), are obtained, which are beyond the current reach of rigorous PDE theory.

The outline of this paper is as follows. In §2 we develop a formal asymptotic approach to construct the asymptotic behaviour of the bifurcation curve to (1.3) in the unit ball in the limit $\varepsilon \equiv 1 - \|u\|_\infty \rightarrow 0^+$. For the unit slab, in §3 we give an explicit characterization of the maximal solution branch for the biharmonic problem (1.1) in the limit $\varepsilon \equiv 1 - \|u\|_\infty \rightarrow 0^+$. Similar results are given for (1.1) in the unit disk in §4. In §5 the limiting asymptotic behaviour of the maximal solution branch to the annulus problem (1.4) is constructed. Finally, a few open problems are discussed in §6.

2 Multiple Fold Points and Singular Asymptotics

In this section, we construct the bifurcation branch of radially symmetric solutions to the generalized membrane problem (1.3) in the limit $\varepsilon \rightarrow 0^+$ where $\|u\|_\infty = 1 - \varepsilon$.

First we consider the slab domain $|x| < 1$ with $N = 1$ for the parameter range $\alpha > \alpha_c$, where $\alpha_c \equiv -1/2 + (3/2)^{3/2}$ is the threshold above which an infinite fold-point structure exists (cf. [23]). By imposing the symmetry condition $u_x(0) = 0$, we consider

$$u_{xx} = \frac{\lambda x^\alpha}{(1+u)^2}, \quad 0 < x < 1; \quad u(1) = u_x(0) = 0, \quad (2.1)$$

in the limit $u(0) + 1 = \varepsilon \rightarrow 0^+$. The nonlinear eigenvalue parameter λ and the outer solution for (2.1), defined away

from $x = 0$, are expanded for $\varepsilon \rightarrow 0$ as

$$u = u_0 + \varepsilon^q u_1 + \dots, \quad \lambda = \lambda_0 + \varepsilon^q \lambda_1 + \dots, \quad (2.2)$$

where $q > 0$ is to be found. In order to match to the inner solution below, the leading-order terms u_0 , λ_0 are taken to be the singular solution of (2.1) for which $u_0(1) = 0$ and $u_0(0) = -1$. This solution is given by

$$u_0 = -1 + x^p, \quad \lambda_0 = p(p-1), \quad p \equiv \frac{\alpha+2}{3}. \quad (2.3)$$

By substituting (2.2) into (2.1), and equating the $\mathcal{O}(\varepsilon^q)$ terms, we obtain that u_1 satisfies

$$\mathcal{L}u_1 \equiv u_{1xx} + \frac{2\lambda_0}{x^2}u_1 = \lambda_1 x^{p-2}, \quad 0 < x < 1; \quad u_1(1) = 0. \quad (2.4)$$

By introducing an inner expansion, valid near $x = 0$, we will derive an appropriate singularity behaviour for u_1 as $x \rightarrow 0$, which will allow for the determination of λ_1 from a solvability condition.

In the inner region near $x = 0$, we introduce the inner variables y and $v(y)$ by

$$y = x/\gamma, \quad u = -1 + \varepsilon v. \quad (2.5)$$

Then, from (2.5) and (2.2) for λ , (2.1) becomes $v'' = \gamma^{2+\alpha}\varepsilon^{-3}y^\alpha[\lambda_0 + \varepsilon^q\lambda_1 + \dots]/v^2$, which suggests the boundary layer width $\gamma = \varepsilon^{1/p}$, where p is defined in (2.3). We then expand v as

$$v = v_0 + \varepsilon^q v_1 + \dots, \quad (2.6)$$

and equate $\mathcal{O}(1)$ and $\mathcal{O}(\varepsilon^q)$ terms in the resulting expression to obtain that v_0 and v_1 satisfy

$$v_0'' = \frac{\lambda_0 y^\alpha}{v_0^2}, \quad 0 < y < \infty; \quad v_0(0) = 1, \quad v_0'(0) = 0, \quad (2.7 a)$$

$$v_1'' + \frac{2\lambda_0 y^\alpha}{v_0^3}v_1 = \frac{\lambda_1 y^\alpha}{v_0^2}, \quad 0 < y < \infty; \quad v_1(0) = v_1'(0) = 0. \quad (2.7 b)$$

The leading-order matching condition is that $v_0 \sim y^p$ as $y \rightarrow \infty$. We linearize about this far field behaviour by writing $v_0 = y^p + w$, where $w \ll y^p$ as $y \rightarrow \infty$, to obtain that w satisfies $w'' + 2\lambda_0 w/y^2 = 0$. By solving this Euler's equation for w explicitly, we obtain that the far-field behaviour of the solution to (2.7 a) is

$$v_0 \sim y^p + Ay^{1/2} \sin(\omega \log y + \phi), \quad \text{as } y \rightarrow \infty, \quad \omega \equiv \frac{1}{2}\sqrt{8\lambda_0 - 1}, \quad (2.8)$$

where A and ϕ are constants depending on α , which must be computed from the numerical solution of (2.7 a) with $v_0 \sim y^p$ as $y \rightarrow \infty$. We remark that $8\lambda_0 - 1 > 0$ when $\alpha > \alpha_c \equiv -1/2 + (3/2)^{3/2}$. In contrast, the far-field behaviour for (2.7 b) is determined by its particular solution. For $y \rightarrow \infty$ we use $v_0 \sim y^p$ in (2.7 b), to obtain

$$v_1 \sim \frac{\lambda_1}{3\lambda_0}y^p, \quad \text{as } y \rightarrow \infty. \quad (2.9)$$

Therefore, by combining (2.8) and (2.9), we obtain the far-field behaviour of the inner expansion $v \sim v_0 + \varepsilon^q v_1$. The matching condition is that this far-field behaviour as $y \rightarrow \infty$ must agree with the near-field behaviour as $x \rightarrow 0$ of the outer expansion in (2.2). By using $u = -1 + \varepsilon v$ and $x = \varepsilon^{1/p}y$, this matching condition yields

$$u \sim -1 + x^p + A\varepsilon^{1-1/(2p)}x^{1/2} \sin\left(\omega \log x - \frac{\omega}{p} \log \varepsilon + \phi\right) + \varepsilon^q \left(\frac{\lambda_1}{3\lambda_0}\right)x^p, \quad \text{as } x \rightarrow 0. \quad (2.10)$$

Therefore, upon comparing (2.10) with the outer expansion for u in (2.2), we conclude that u_1 must solve (2.4), subject to the singular behaviour

$$u_1 \sim Ax^{1/2} \sin(\omega \log x + \phi_\varepsilon) + \frac{\lambda_1}{3\lambda_0}x^p, \quad \text{as } x \rightarrow 0, \quad (2.11)$$

where we have defined the exponent q and the phase ϕ_ε by $q = 1 - 1/(2p)$ and $\phi_\varepsilon \equiv -\omega p^{-1} \log \varepsilon + \phi$.

Next, we solve the problem (2.4) for u_1 , with singular behaviour (2.11). Since the first term in the asymptotic behaviour in (2.11) is a solution to the homogeneous problem in (2.4), while the second term is the particular solution for (2.4), it is convenient to decompose u_1 as

$$u_1 = \frac{\lambda_1}{3\lambda_0} x^p + Ax^{1/2} \sin(\omega \log x + \phi_\varepsilon) + U_{1a}, \quad (2.12)$$

to obtain that U_{1a} solves

$$\mathcal{L}U_{1a} = 0, \quad 0 < x < 1; \quad U_{1a}(1) = -\frac{\lambda_1}{3\lambda_0} - A \sin \phi_\varepsilon; \quad U_{1a} = o(x^{1/2}), \quad \text{as } x \rightarrow 0. \quad (2.13)$$

To determine λ_1 we apply a solvability condition. The function $\Phi = x^{1/2} \sin(\omega \log x + k\pi)$ is a solution to $\mathcal{L}\Phi = 0$ with $\Phi(1) = 0$ for any integer k , and has the asymptotic behaviour $\Phi = \mathcal{O}(x^{1/2})$ and $\Phi_x = \mathcal{O}(x^{-1/2})$ as $x \rightarrow 0$. By applying Lagrange's identity to U_{1a} and Φ over the interval $0 < \sigma < x < 1$, and by using $\Phi(1) = 0$, we obtain

$$0 = \int_\sigma^1 (\phi \mathcal{L}U_{1a} - U_{1a} \mathcal{L}\Phi) dx = -U_{1a}(1)\Phi_x(1) - [\Phi U_{1ax} - U_{1a}\Phi_x]_{x=\sigma}. \quad (2.14)$$

Finally, we take the limit $\sigma \rightarrow 0$ in (2.14) and use $U_{1a} = o(x^{1/2})$, $U_{1ax} = o(x^{-1/2})$, and $\Phi_x(1) \neq 0$, as $x \rightarrow 0$. This yields $U_{1a}(1) = 0$, which determines $\lambda_1 = -3A\lambda_0 \sin \phi_\varepsilon$ from (2.13). We summarize our asymptotic result as follows:

Principal Result 2.1: For $\varepsilon \equiv u(0) + 1 \rightarrow 0^+$ and $\alpha > \alpha_c \equiv -1/2 + (3/2)^{3/2}$ a two-term asymptotic expansion for the bifurcation curve λ versus ε of (2.1) is given by

$$\lambda \sim \lambda_0 + 3A\lambda_0 \varepsilon^q \sin\left(\frac{3\omega}{2+\alpha} \log \varepsilon - \phi\right) + \dots, \quad (2.15 a)$$

where q , ω , and λ_0 , are defined by

$$q = 1 - \frac{3}{2(\alpha+2)}, \quad \omega = \frac{1}{2} \sqrt{8\lambda_0 - 1}, \quad \lambda_0 = \frac{(\alpha-1)(\alpha+2)}{9}. \quad (2.15 b)$$

The constants A and ϕ , which depend on α , are determined numerically from the solution to (2.7 a) with far-field behaviour (2.8). These constants are given in the first row of Table 1 for a few values of α . The asymptotic prediction for the locations of the infinite sequence of fold points, determined by setting $d\lambda/d\varepsilon = 0$, is

$$u(0) = -1 + \varepsilon_m, \quad \varepsilon_m = \exp\left[\frac{(\alpha+2)}{3\omega} \left(\phi - \frac{(2m-1)\pi}{2}\right)\right], \quad \lambda_m = \lambda_0 + 3\lambda_0 A \varepsilon_m^q (-1)^m, \quad m = 1, 2, \dots \quad (2.15 c)$$

These fold points are such that the difference $u(0) + 1$ is exponentially small as $\varepsilon \rightarrow 0$.

We remark that the analysis leading to Principal Result 2.1 is non-standard as a result of two features. Firstly, the correction term u_1 in the outer expansion for u is not independent of ε , but in fact depends on $\log \varepsilon$. However, although u_1 is weakly oscillatory in ε , it is uniformly bounded as $\varepsilon \rightarrow 0$. Secondly, the solvability condition determining λ_1 pertains to a countably infinite sequence of functions $\Phi = x^{1/2} \sin(\omega \log x + k\pi)$ where k is an integer.

2.1 Infinite Number of Fold Points for $N > 1$

Next, we use a similar analysis to determine the limiting form of the bifurcation diagram for radially symmetric solutions of (1.3) in the N -dimensional unit ball. To this end, the solution branches of

$$u_{rr} + \frac{(N-1)}{r} u_r = \frac{\lambda r^\alpha}{(1+u)^2}, \quad 0 < r < 1; \quad u(1) = 0, \quad u_r(0) = 0, \quad (2.16)$$

will be constructed asymptotically in the limit $u(0) + 1 = \varepsilon \rightarrow 0^+$, where $\alpha \geq 0$ and $N \geq 2$. For $N = 2$, the term r^α represents a variable dielectric permittivity of the membrane (cf. [23], [10]).

In the limit $\varepsilon \rightarrow 0$, (2.16) is a singular perturbation problem with an outer region, where $\mathcal{O}(\gamma) < r < 1$ with $u = \mathcal{O}(1)$, and an inner region with $r = \mathcal{O}(\gamma)$ and $u = \mathcal{O}(\varepsilon)$. Here $\gamma \ll 1$ is the boundary layer width to be found in terms of ε . The nonlinear eigenvalue parameter λ and the outer solution are expanded as

$$u \sim u_0 + \varepsilon^q u_1 + \dots, \quad \lambda \sim \lambda_0 + \varepsilon^q \lambda_1 + \dots, \quad (2.17)$$

for some $q > 0$ to be determined. For the leading-order problem for u_0 and λ_0 , a singular solution of (2.16) is constructed for which $u_0(0) = -1$. This singular solution is given explicitly by

$$u_0 = -1 + r^p, \quad \lambda_0 = p^2 + (N-2)p, \quad p \equiv \frac{(\alpha+2)}{3}. \quad (2.18)$$

The substitution of (2.17) into (2.16), together with using (2.18) for u_0 , shows that u_1 satisfies

$$\mathcal{L}_N u_1 \equiv u_1'' + \frac{(N-1)}{r} u_1' + \frac{2\lambda_0}{r^2} u_1 = \lambda_1 r^{p-2}, \quad 0 < r < 1; \quad u_1(1) = 0. \quad (2.19)$$

The required singularity behaviour for u_1 as $r \rightarrow 0$ will be determined below by matching u_1 to the inner solution.

In the inner region near $r = 0$, we introduce the inner variables v and ρ and the inner expansion by

$$u = -1 + \varepsilon v, \quad v = v_0 + \varepsilon^q v_1 + \dots, \quad \rho = r/\gamma, \quad \gamma = \varepsilon^{1/p}. \quad (2.20)$$

By substituting (2.20) into (2.16), we obtain that $v_0(\rho)$ and $v_1(\rho)$ satisfy

$$v_0'' + \frac{(N-1)}{\rho} v_0' = \frac{\lambda_0 \rho^\alpha}{v_0^2}, \quad 0 < \rho < \infty; \quad v_0(0) = 1, \quad v_0'(\infty) = 0, \quad (2.21 a)$$

$$v_1'' + \frac{(N-1)}{\rho} v_1' + \frac{2\lambda_0 \rho^\alpha}{v_0^3} v_1 = \frac{\lambda_1 \rho^\alpha}{v_0^2}, \quad 0 < \rho < \infty; \quad v_1(0) = v_1'(\infty) = 0. \quad (2.21 b)$$

The leading-order matching condition is that $v_0 \sim \rho^p$ as $\rho \rightarrow \infty$. We linearize about this far field behaviour by writing $v_0 = \rho^p + w$, where $w \ll \rho^p$ as $\rho \rightarrow \infty$, to obtain that w satisfies

$$w'' + \frac{(N-1)}{\rho} w' + \frac{2\lambda_0}{\rho^2} w = 0. \quad (2.22)$$

A solution to this Euler equation is

$$w = \rho^\mu, \quad \mu = -\frac{(N-2)}{2} \pm \frac{\sqrt{(N-2)^2 - 8\lambda_0}}{2}. \quad (2.23)$$

This leads to two different cases, depending on whether $(N-2)^2 > 8\lambda_0$ or $(N-2)^2 < 8\lambda_0$.

We first consider the case where $(N-2)^2 < 8\lambda_0$, for which μ is complex. As shown below, this is the case where the bifurcation diagram of λ versus ε has an infinite number of fold points. For this case, the explicit solution for w leads to the following far-field behaviour for the solution v_0 of (2.21 a):

$$v_0 = \rho^p + A \rho^{1-N/2} \sin(\omega_N \log \rho + \phi) + o(1), \quad \text{as } \rho \rightarrow \infty; \quad \omega_N \equiv \frac{1}{2} \sqrt{8\lambda_0 - (N-2)^2}. \quad (2.24)$$

Here the constants A and ϕ , depending on N and α , must be computed numerically from the solution to (2.21 a) with far-field behaviour (2.24). In Table 1 numerical values for these constants are given for different α and N for the parameter range where $(N-2)^2 < 8\lambda_0$. The results for A and ϕ are also plotted in Fig. 5(a). In particular, for $N = 2$ and $\alpha = 0$,

$$A = 0.4727, \quad \phi = 3.2110. \quad (2.25)$$

N	$\alpha = 0$		$\alpha = 1$		$\alpha = 2$		$\alpha = 3$		$\alpha = 4$	
	A	ϕ	A	ϕ	A	ϕ	A	ϕ	A	ϕ
1	–	–	–	–	1.1678	3.9932	0.8713	3.7029	0.7563	3.5816
2	0.4727	3.2110	0.4727	3.2110	0.4727	3.2110	0.4727	3.2110	0.4727	3.2110
3	0.2454	2.5050	0.2864	2.7231	0.3152	2.8351	0.3363	2.9042	0.3528	2.9519
4	0.1935	1.8789	0.2193	2.2932	0.2454	2.5048	0.2676	2.6347	0.2862	2.7224
5	0.1972	1.2755	0.1935	1.8790	0.2101	2.1886	0.2284	2.3775	0.2454	2.5050
6	0.2586	0.7008	0.1909	1.4743	0.1935	1.8790	0.2056	2.1262	0.2194	2.2927
7	0.4859	0.1945	0.2095	1.0803	0.1896	1.5746	0.1935	1.8790	0.2029	2.0852

Table 1. Numerical values of A and ϕ for different exponents α and dimension N computed from the far-field behaviour of the solution to (2.21 a) with (2.24).

For $N = 2$ and $\alpha = 0$, in Fig. 5(b) the numerically computed far-field behaviour of v_0 is plotted after subtracting off the $\mathcal{O}(\rho^{2/3})$ algebraic growth at infinity. Indeed, this far-field behaviour is oscillatory as predicted by (2.24).

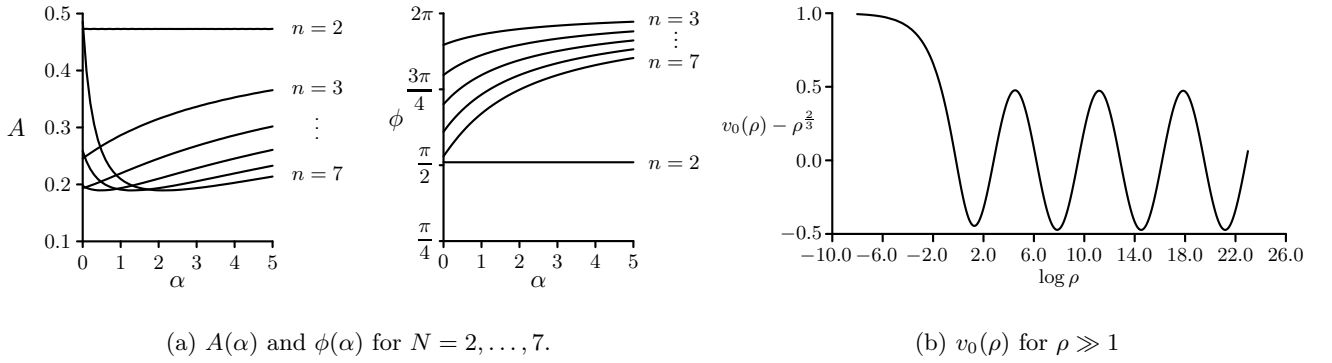


FIGURE 5. Left figure: numerical results for the far-field constants A and ϕ in (2.24) for different N and α . Right figure: Plot of $v_0 - \rho^{2/3}$ versus $\log \rho$ as computed numerically from (2.21 a) for $N = 2$ and $\alpha = 0$. The far-field behaviour is oscillatory.

For v_1 , the far-field behaviour for (2.21 b) is determined by its particular solution. For $y \rightarrow \infty$ we use $v_0 \sim y^p$ in (2.21 b), to obtain

$$v_1 \sim \frac{\lambda_1}{3\lambda_0} \rho^p, \quad \text{as } \rho \rightarrow \infty. \quad (2.26)$$

Therefore, by combining (2.24) and (2.26), we obtain the far-field behaviour of the inner expansion $v \sim v_0 + \varepsilon^q v_1$. The matching condition is that this far-field behaviour as $\rho \rightarrow \infty$ must agree with the near-field behaviour as $x \rightarrow 0$ of the outer expansion in (2.17). By using $u = -1 + \varepsilon v$ and $r = \varepsilon^{1/p} \rho$, and by choosing the exponent q in (2.17) appropriately, we obtain that u_1 must solve (2.19) subject to the singular behaviour

$$u_1 \sim A r^{1-N/2} \sin(\omega_N \log r + \phi_\varepsilon) + \frac{\lambda_1}{3\lambda_0} r^p, \quad \text{as } r \rightarrow 0, \quad (2.27)$$

where q and ϕ_ε are defined by

$$q \equiv 1 + \frac{3}{2} \left(\frac{N-2}{\alpha+2} \right), \quad \phi_\varepsilon = -\frac{3\omega_N}{\alpha+2} \log \varepsilon + \phi. \quad (2.28)$$

Next, we solve the problem (2.19) subject to the singular behaviour (2.27). To do so, we decompose u_1 as

$$u_1 = \frac{\lambda_1}{3\lambda_0} r^p + A r^{1-N/2} \sin(\omega_N \log r + \phi_\varepsilon) + U_{1a}, \quad (2.29)$$

to obtain that U_{1a} solves

$$\mathcal{L}_N U_{1a} = 0, \quad 0 < r < 1; \quad U_{1a}(1) = -\frac{\lambda_1}{3\lambda_0} - A \sin \phi_\varepsilon; \quad U_{1a} = o(r^{1-N/2}), \quad \text{as } r \rightarrow 0. \quad (2.30)$$

Since the solution to the homogeneous problem is $\Phi = r^{1-N/2} \sin(\omega_N \log r + k\pi)$ for any integer $k \geq 0$, then Green's second identity is readily used to obtain a solvability condition for (2.30). The application of this identity to U_{1a} and Φ on the interval $\sigma \leq r \leq 1$ yields

$$0 = \int_\sigma^1 r^{N-1} (\Phi \mathcal{L}_N U_{1a} - U_{1a} \mathcal{L}_N \Phi) dr = -r^{N-1} (\Phi \partial_r U_{1a} - U_{1a} \partial_r \Phi) \Big|_{r=\sigma}^{r=1}. \quad (2.31)$$

Since $\Phi(1) = 0$, the passage to the limit $\sigma \rightarrow 0$ in (2.31) results in

$$U_{1a} \partial_r \Phi|_{r=1} = -\lim_{\sigma \rightarrow 0} \sigma^{N-1} (\Phi \partial_r U_{1a} - U_{1a} \partial_r \Phi) \Big|_{r=\sigma}. \quad (2.32)$$

Now since $U_{1a} = o(r^{1-N/2})$, $\partial_r U_{1a} = o(r^{-N/2})$, $\Phi = \mathcal{O}(r^{1-N/2})$, and $\partial_r \Phi = \mathcal{O}(r^{-N/2})$ as $r \rightarrow 0$, there is no contribution in (2.32) from the limit $\sigma \rightarrow 0$. Consequently, $U_{1a}(1) = 0$, which determines λ_1 as $\lambda_1 = -3\lambda_0 A \sin \phi_\varepsilon$ from (2.30). We summarize our asymptotic result as follows:

Principal Result 2.2: For $\varepsilon \equiv u(0) + 1 \rightarrow 0^+$ assume that $2 < N < N_c$ and $\alpha \geq 0$, where

$$N_c \equiv 2 + \frac{4(\alpha + 2)}{3} + \frac{2\sqrt{6}}{3}(\alpha + 2). \quad (2.33)$$

Then a two-term asymptotic expansion for the bifurcation curve λ versus ε for (2.16) is given by

$$\lambda \sim \lambda_0 + 3\varepsilon^q A \lambda_0 \sin\left(\frac{3\omega_N}{\alpha + 2} \log \varepsilon - \phi\right), \quad (2.34 a)$$

where q is defined in (2.28). The constants A and ϕ , depending on N and α , are given in Table 1 and Fig. 5(a), and were computed numerically from the solution to (2.21 a) with far-field behaviour (2.24). The asymptotic prediction for the locations of the infinite sequence of fold points, determined by setting $d\lambda/d\varepsilon = 0$, is

$$u(0) = -1 + \varepsilon_m, \quad \varepsilon_m = \exp\left[\frac{(\alpha + 2)}{3\omega_N} \left(\phi - \frac{(2m-1)\pi}{2}\right)\right], \quad \lambda_m = \lambda_0 + 3\lambda_0 A \varepsilon_m^q (-1)^m, \quad m = 1, 2, \dots, \quad (2.34 b)$$

where ω_N is defined in (2.24).

The condition on N in (2.33) is both necessary and sufficient to guarantee that $8\lambda_0 > (N-2)^2$. For $\alpha = 0$, (2.33) yields that the dimension N satisfies $2 \leq N \leq 7$. For any $N \geq 8$, it follows from (2.33) that (2.16) has an infinite number of fold points if $\alpha > \alpha_{cN}$, where α_{cN} is defined by

$$\alpha_{cN} \equiv -2 + \frac{3(N-2)}{4 + 2\sqrt{6}}. \quad (2.35)$$

From Table 1 and Fig. 5(a) it appears that A and ϕ are independent of α when $N = 2$. This result follows analytically by using a change of variables motivated by that in [3]. We introduce the new variables $\rho = y^{1+\alpha/2}$ and $V_0(y) = v_0 [y^{1+\alpha/2}]$. Then, (2.21 a) and (2.24) transform to the following problem for $V_0(y)$:

$$V_0'' + \frac{1}{y} V_0' = \frac{\tilde{\lambda}_0}{V_0^2}, \quad 0 < y < \infty; \quad V_0(0) = 1, \quad V_0'(0) = 0; \quad V_0 \sim y^{2/3} + A \sin\left[\frac{2\sqrt{2}}{3} \log y + \phi\right], \quad \text{as } y \rightarrow \infty,$$

with $\tilde{\lambda}_0 \equiv \lambda_0 / (1 + \alpha/2)^2$. This problem is precisely (2.21 a) and (2.24) for the special case where $\alpha = 0$. Thus, when $N = 2$ and for any $\alpha > 0$, the constants A and ϕ are given by their numerically computed values obtained for $\alpha = 0$.

Next, we consider the case where $8\lambda_0 < (N-2)^2$, for which $N > N_c$. For this case, the solution v_0 to (2.21 a) has

the far-field behaviour

$$v_0 \sim \rho^p + \mathcal{A}\rho^{\mu_+}, \quad \text{as } \rho \rightarrow \infty; \quad \mu_+ \equiv 1 - \frac{N}{2} + \frac{\sqrt{(N-2)^2 - 8\lambda_0}}{2}, \quad (2.36)$$

for some constant \mathcal{A} , depending on N and α , which must be calculated numerically. A simple calculation shows that $p > \mu_+$. In addition, the far-field behaviour of the solution v_1 to (2.21 b) has the asymptotic behaviour in (2.26).

Then, by using $u = -1 + \varepsilon v$ and $r = \varepsilon^{1/p}\rho$, where $v = v_0 + \varepsilon^q v_1$, and by choosing the exponent q in (2.17) appropriately, we obtain that u_1 must solve (2.19) subject to the singular behaviour

$$u_1 \sim \mathcal{A}r^{\mu_+} + \frac{\lambda_1}{3\lambda_0}r^p, \quad \text{as } r \rightarrow 0, \quad (2.37)$$

where $q = 1 - 3\mu_+/(2 + \alpha)$. Upon decomposing u_1 as

$$u_1 = \mathcal{A}r^{\mu_+} + \frac{\lambda_1}{3\lambda_0}r^p + U_{1a}, \quad (2.38)$$

we obtain from (2.19) that U_{1a} solves

$$\mathcal{L}_N U_{1a} = 0, \quad 0 < r < 1; \quad U_{1a}(1) = -\frac{\lambda_1}{3\lambda_0} - \mathcal{A}; \quad U_{1a} = o(r^{\mu_+}), \quad \text{as } r \rightarrow 0. \quad (2.39)$$

The solvability condition for this problem determines λ_1 as $\lambda_1 = -3\lambda_0\mathcal{A}$. We summarize our result as follows:

Principal Result 2.3: For $\varepsilon \equiv u(0) + 1 \rightarrow 0^+$ assume that $N > N_c$, where N_c is defined in (2.33). Then, a two-term asymptotic expansion for the bifurcation curve λ versus ε for (2.16) is given by

$$u(0) = -1 + \varepsilon, \quad \lambda \sim \lambda_0 - 3\varepsilon^q \mathcal{A}\lambda_0, \quad (2.40)$$

where $q = 1 - 3\mu_+/(2 + \alpha)$ and μ_+ is defined in (2.36). The constant \mathcal{A} , which depends on α and N , must be computed numerically from the solution to (2.21 a) with far-field behaviour (2.36).

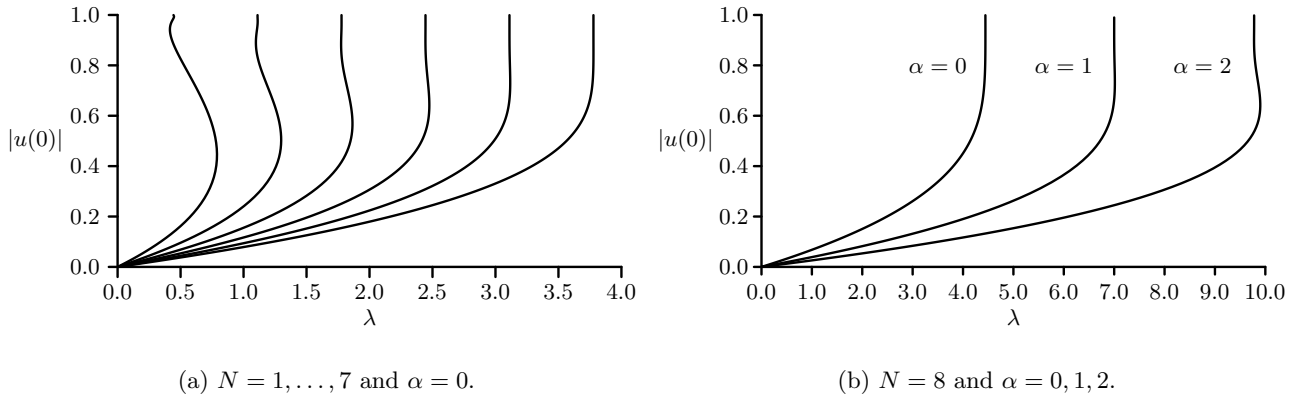


FIGURE 6. Left figure: numerical bifurcation curves $|u(0)|$ versus λ for $N = 1, \dots, 7$ and $\alpha = 0$. Right figure: numerical bifurcation curves for $N = 8$ and $\alpha = 0, 1, 2$. The results were computed numerically from (2.16).

In Fig. 6 plots are shown for the bifurcation diagrams of $|u(0)|$ versus λ , as computed numerically from (2.16) for $N = 1, \dots, 7$ and $\alpha = 0$ (see Fig. 6(a)) and for $N = 8$ with $\alpha = 0, 1, 2$ (see Fig. 6(b)). For representative values of N and α , in Fig. 7 it is observed that the asymptotic results for the bifurcation diagram as obtained from either (2.34) or (2.40) closely approximate the numerically computed bifurcation curves of (2.16).

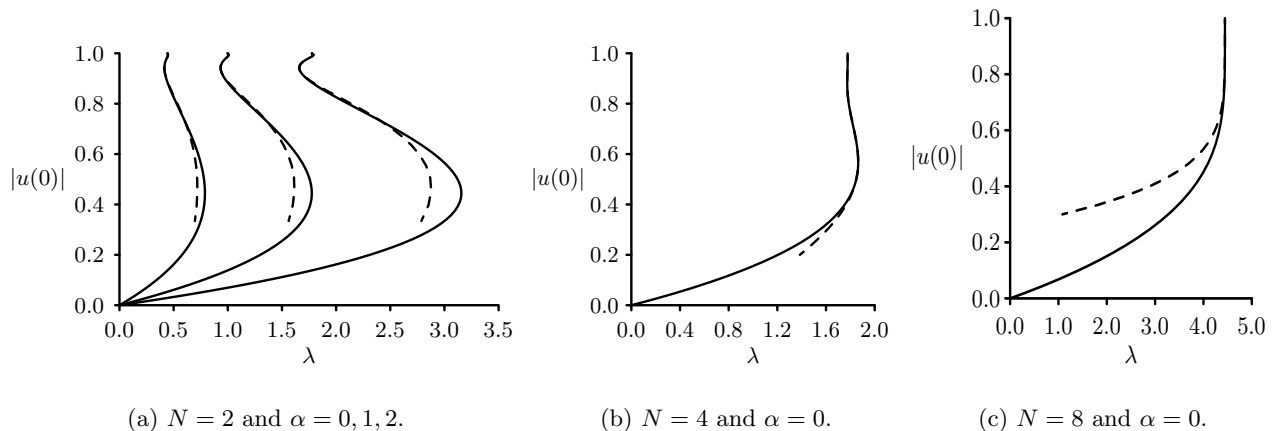


FIGURE 7. Comparison of bifurcation curves for $N = 2$ with $\alpha = 0, 1, 2$ (left figure), $N = 4$ and $\alpha = 0$ (middle figure), and $N = 8$ with $\alpha = 0$ (right figure). The solid curves are the full numerical results and the dashed curves are the asymptotic results obtained from either (2.34) or (2.40).

We remark that the thresholds N_c and α_{cN} of (2.33) and (2.35) were previously identified in the rigorous studies of [12], [8], and [5], of the infinite fold-point structure for (2.16). The results in Principal Results 2.1 and 2.2, determined in terms of two constants that must be computed, provide the first *explicit* asymptotic representation of the limiting form of the infinite fold-point structure.

3 Asymptotics of the Maximal Solution Branch as $\lambda \rightarrow 0$: The Slab Domain

In this section we use the method of matched asymptotic expansions to construct the limiting asymptotic behaviour of the maximal solution branch for the biharmonic problem (1.1) in a slab domain. To illustrate the analysis, we first consider the pure biharmonic nonlinear eigenvalue problem

$$-u_{xxxx} = \frac{\lambda}{(1+u)^2}, \quad -1 < x < 1; \quad u(\pm 1) = u_x(\pm 1) = 0, \quad (3.1)$$

in the limit where $\varepsilon \equiv u(0) + 1 \rightarrow 0^+$. We assume that $\lambda_\varepsilon \rightarrow 0$ as $\varepsilon \rightarrow 0^+$, so that in terms of some $\nu(\varepsilon) \ll 1$,

$$\lambda_\varepsilon \sim \nu(\varepsilon)\lambda_0 + \dots. \quad (3.2)$$

Since u_ε is even in x , we restrict (3.1) to $0 < x < 1$ and impose the symmetry conditions $u_x(0) = u_{xxx}(0) = 0$.

In the outer region for $0 < x < 1$, we expand the solution as

$$u_\varepsilon \sim u_0 + \nu(\varepsilon)u_1 + \dots. \quad (3.3)$$

From (3.3) and (3.1), we obtain on $0 < x < 1$ that

$$u_{0xxxx} = 0, \quad 0 < x < 1; \quad u_0(1) = u_{0x}(1) = 0, \quad (3.4a)$$

$$u_{1xxxx} = -\frac{\lambda_0}{(1+u_0)^2}, \quad 0 < x < 1; \quad u_1(1) = u_{1x}(1) = 0. \quad (3.4b)$$

For (3.4a), we impose the point constraints $u_0(0) = -1$ and $u_{0x}(0) = 0$ in order to match to an inner solution below. This determines $u_0(x)$ as

$$u_0(x) = -1 + 3x^2 - 2x^3. \quad (3.5)$$

Since $u_{0xxx}(0) \neq 0$, u_0 does not satisfy the symmetry condition $u_{xxx}(0) = 0$. Thus, we need an inner layer near $x = 0$.

Upon substituting (3.5) into (3.4 b), we obtain for $x \ll 1$ that

$$u_{1xxxx} = -\frac{\lambda_0}{(3x^2 - 2x^3)^2} = -\frac{\lambda_0}{9x^4} \left(1 - \frac{2x}{3}\right)^{-2} \sim -\frac{\lambda_0}{9x^4} \left(1 + \frac{4x}{3} + \frac{12x^2}{9} + \dots\right).$$

Then, by integrating this limiting relation, we obtain the local behaviour

$$u_1 \sim \frac{\lambda_0}{54} \log x - \frac{2\lambda_0}{27} x \log x + c_1 + b_1 x + \mathcal{O}(x^2 \log x), \quad \text{as } x \rightarrow 0, \quad (3.6)$$

in terms of constants c_1 and b_1 to be determined. By determining these constants, which then specifies the homogeneous solution for u_1 , the solution u_1 can be found uniquely. From (3.3), (3.5), and (3.6), we obtain that

$$u_\varepsilon \sim -1 + 3x^2 - 2x^3 + \nu \left(\frac{\lambda_0}{54} \log x - \frac{2\lambda_0}{27} x \log x + c_1 + b_1 x + \mathcal{O}(x^2 \log x) \right) + \dots, \quad \text{as } x \rightarrow 0. \quad (3.7)$$

By introducing the inner variable $y = x/\gamma$, we have to leading order from (3.7) that $u \sim -1 + 3\gamma^2 y^2 + \dots$ as $x \rightarrow 0$. Since $u = -1 + \mathcal{O}(\varepsilon)$ in the inner region, this motivates the scaling of the local variables y and v defined by

$$y = x/\varepsilon^{1/2}, \quad u = -1 + \varepsilon v(y). \quad (3.8)$$

Next, we balance the cubic term $-2x^3$ in (3.7) with the $\mathcal{O}(\nu)$ term in (3.7) to get $\nu = \varepsilon^{3/2}$. Then, we substitute (3.8) and $\lambda_\varepsilon \sim \varepsilon^{3/2} \lambda_0$ into (3.1), to obtain that $v(y)$ satisfies

$$-v'''' = \varepsilon^{1/2} \frac{[\lambda_0 + \dots]}{v^2}, \quad 0 < y < \infty; \quad v(0) = 1, \quad v'(0) = v'''(0) = 0. \quad (3.9)$$

To determine the correct expansions for the inner and outer solutions, we write the local behaviour of the outer expansion in (3.7) in terms of the inner variable $x = \varepsilon^{1/2} y$, with $\nu = \varepsilon^{3/2}$, to get

$$u_\varepsilon = -1 + 3\varepsilon y^2 + \left(\varepsilon^{3/2} \log \varepsilon\right) \frac{\lambda_0}{108} + \varepsilon^{3/2} \left(-2y^3 + \frac{\lambda_0}{54} \log y + c_1\right) + (-\varepsilon^2 \log \varepsilon) \frac{\lambda_0}{27} y + \varepsilon^2 \left[-\frac{2\lambda_0}{27} y \log y + b_1 y\right] + \mathcal{O}(\varepsilon^{5/2} \log \varepsilon). \quad (3.10)$$

The terms of order $\mathcal{O}(\varepsilon^{3/2} \log \varepsilon)$ and order $\mathcal{O}(\varepsilon^2 \log \varepsilon)$ can be removed with a switchback term in the outer expansion. In addition, from the $\mathcal{O}(\varepsilon)$ term in (3.10), we conclude from (3.9) that $v \sim v_0 + o(1)$, where v_0 satisfies

$$v'''' = 0, \quad 0 < y < \infty; \quad v_0(0) = 1, \quad v'_0 = v'''_0(0) = 0; \quad v_0 \sim 3y^2 \quad \text{as } y \rightarrow \infty, \quad (3.11 a)$$

which has the exact solution is

$$v_0 = 3y^2 + 1. \quad (3.11 b)$$

The constant term in (3.11 b) then generates the unmatched term ε in the outer region, which can only be removed by introducing a second switchback term into the outer expansion.

This suggests that λ_ε , and the outer expansion for u_ε , must have the form

$$u_\varepsilon = u_0 + \varepsilon u_{1/2} + \left(\varepsilon^{3/2} \log \varepsilon\right) u_{3/2} + \varepsilon^{3/2} u_1 + \dots, \quad \lambda_\varepsilon = \varepsilon^{3/2} \lambda_0 + \varepsilon^2 \lambda_1 + \dots. \quad (3.12)$$

Upon substituting (3.12) into (3.1), and collecting similar terms in ε , we obtain that $u_{1/2}$ satisfies

$$u_{1/2xxxx} = 0, \quad 0 < x < 1; \quad u_{1/2}(0) = 1, \quad u_{1/2x}(0) = b_{1/2}, \quad u_{1/2}(1) = u_{1/2x}(1) = 0, \quad (3.13 a)$$

where $b_{1/2}$ is a constant to be found. The condition $u_{1/2}(0) = 1$ accounts for the constant term in v_0 . The solution is

$$u_{1/2}(x) = 1 + b_{1/2} x + (-3 - 2b_{1/2}) x^2 + (b_{1/2} + 2) x^3. \quad (3.13 b)$$

Similarly, $u_{3/2}(x)$ satisfies $u_{3/2xxxx} = 0$. To eliminate the $\mathcal{O}(\varepsilon^{3/2} \log \varepsilon)$ and $\mathcal{O}(\varepsilon^2 \log \varepsilon)$ terms in (3.10), we let $u_{3/2}$ satisfy

$$u_{3/2xxxx} = 0, \quad 0 < x < 1; \quad u_{3/2}(0) = -\frac{\lambda_0}{108}, \quad u_{3/2x}(0) = \frac{\lambda_0}{27}, \quad u_{3/2}(1) = u_{3/2x}(1) = 0. \quad (3.14 a)$$

The solution for $u_{3/2}$ is

$$u_{3/2} = \lambda_0 \left(-\frac{1}{108} + \frac{x}{27} - \frac{5x^2}{108} + \frac{x^3}{54} \right). \quad (3.14 b)$$

We then substitute (3.5), (3.6), (3.13 b), (3.14 b), for u_0 , u_1 , $u_{1/2}$, and $u_{3/2}$ respectively, into the outer expansion (3.12), and we write the resulting expression in terms of the inner variable $x = \varepsilon^{1/2}y$. This yields the following behaviour for u_ε as $x \rightarrow 0$:

$$u \sim -1 + \varepsilon(3y^2 + 1) + \varepsilon^{3/2} \left(-2y^3 + \frac{\lambda_0}{54} \log y + b_{1/2}y + c_1 \right) + \varepsilon^2 \left(-(3 + 2b_{1/2})y^2 - \frac{2\lambda_0}{27}y \log y + b_1y + \dots \right). \quad (3.15)$$

The local behaviour (3.15) suggests that we expand the inner solution as

$$v = v_0 + \varepsilon^{1/2}v_1 + \varepsilon v_2 + \dots. \quad (3.16)$$

Upon substituting (3.16) and (3.12) for λ_ε into (3.9), we obtain that v_0 satisfies (3.11), and that v_1 satisfies

$$v_1'''' = -\frac{\lambda_0}{v_0^2}, \quad 0 < y < \infty; \quad v_1(0) = v_1'(0) = v_1'''(0) = 0, \quad (3.17 a)$$

$$v_1 \sim -2y^3 + \frac{\lambda_0}{54} \log y + b_{1/2}y + c_1, \quad \text{as } y \rightarrow \infty, \quad (3.17 b)$$

while v_2 satisfies

$$v_2'''' = \frac{2\lambda_0}{v_0^3}v_1 - \frac{\lambda_1}{v_0^2}, \quad 0 < y < \infty; \quad v_2(0) = v_2'(0) = v_2'''(0) = 0, \quad (3.18 a)$$

$$v_2 \sim -(3 + 2b_{1/2})y^2 - \frac{2\lambda_0}{27}y \log y + b_1y + \dots, \quad \text{as } y \rightarrow \infty. \quad (3.18 b)$$

The solution to these problems determine λ_0 , λ_1 , $b_{1/2}$, c_1 and b_1 , as we now show.

To determine λ_0 we use $v_0 = (3y^2 + 1)$ and integrate (3.17 a) for v_0 from $0 < y < R$ to get

$$\lim_{R \rightarrow \infty} v_1'''' \Big|_0^R = -\lambda_0 \int_0^\infty \frac{1}{(3y^2 + 1)^2} dy = -\frac{\lambda_0}{9} \int_0^\infty \frac{1}{(y^2 + 1/3)^2} dy = -\frac{\lambda_0}{9} \left(\frac{3^{3/2}\pi}{4} \right) = -\frac{\sqrt{3}\pi \lambda_0}{12}.$$

Then, by using the limiting behaviour $v_1 \sim -2y^3$ as $y \rightarrow \infty$, we determine λ_0 as $\lambda_0 = 48\sqrt{3}/\pi$.

Next, we calculate $b_{1/2}$ directly from (3.17). To do so, we use Green's second identity to obtain

$$\lim_{R \rightarrow \infty} \int_0^R (v_0 v_1'''' - v_1 v_0'''') dy = \lim_{R \rightarrow \infty} (v_0 v_1'''' - v_0' v_1''' + v_0'' v_1'' - v_0''' v_1) \Big|_0^R.$$

Then, upon using $v_0(y) = 3y^2 + 1$, together with the problem (3.17) for v_1 , we obtain that

$$\begin{aligned} \lim_{R \rightarrow \infty} \int_0^R v_0 v_1'''' dy &= \lim_{R \rightarrow \infty} [(3R^2 + 1)(-12) - 6R(-12R) + 6(-6R^2 + b_{1/2}) + \dots], \\ -\lambda_0 \lim_{R \rightarrow \infty} \int_0^R \frac{1}{v_0} dy &= -\lambda_0 \int_0^\infty \frac{1}{3y^2 + 1} dy = -12 + 6b_{1/2}. \end{aligned} \quad (3.19)$$

Upon evaluating the integral, and then using $\lambda_0 = 48\sqrt{3}/\pi$, we obtain from (3.19) that $b_{1/2} = -2$.

Next, to determine c_1 in (3.17), we first must calculate $v_1''(0)$ and then write (3.17) as an initial value ODE problem

for v_1 . To do so, we multiply (3.17) by v'_0 , and integrate over $0 < y < R$, to get

$$\begin{aligned} \lim_{R \rightarrow \infty} \int_0^R v'_0 v_1'''' dy &= \lim_{R \rightarrow \infty} (v'_0 v_1'''' - v_0'' v_1'') \Big|_0^R + \lim_{R \rightarrow \infty} \int_0^R v_1'' v_0'''' dy, \\ -\lambda_0 \lim_{R \rightarrow \infty} \int_0^R \frac{v'_0}{v_0^2} dy &= v_0''(0) v_1''(0) + \lim_{R \rightarrow \infty} [6R(-12) - 6(-12R) + \dots], \\ \lambda_0 \lim_{R \rightarrow \infty} \left(\frac{1}{v_0} \right) \Big|_{v_0=1}^\infty &= 6v_1''(0). \end{aligned} \quad (3.20)$$

Since $v_0(0) = 1$, this yields that $v_1''(0) = -\lambda_0/6$. Then, with the initial values $v_1(0) = v_1'(0) = v_1''(0) = 0$, and $v_1''(0) = -\lambda_0/6$, we can solve the initial value problem (3.17) for v_1 to obtain

$$v_1 = -\frac{\lambda_0}{12\sqrt{3}} y^3 \tan^{-1}(\sqrt{3}y) - \frac{\lambda_0}{36} y^2 + \frac{\lambda_0}{108} \log(1+3y^2) - \frac{\lambda_0}{12\sqrt{3}} y \tan^{-1}(\sqrt{3}y). \quad (3.21)$$

Upon using the large argument expansion $\tan^{-1}(z) \sim \pi/2 - z^{-1} + (3z^3)^{-1}$ for $z \rightarrow \infty$ in (3.21), we calculate that

$$v_1 \sim -\frac{\lambda_0 \pi}{24\sqrt{3}} y^3 + \frac{\lambda_0}{54} \log y - \frac{\lambda_0 \pi}{24\sqrt{3}} y + \frac{2\lambda_0}{81} + \frac{\lambda_0 \log 3}{108}, \quad \text{as } y \rightarrow \infty. \quad (3.22)$$

Since $\lambda_0 = 48\sqrt{3}/\pi$, we compare (3.22) with the required far-field behaviour for v_1 in (3.17 b), to determine c_1 as

$$c_1 = \lambda_0 \left(\frac{2}{81} + \frac{\log 3}{108} \right), \quad \lambda_0 = \frac{48\sqrt{3}}{\pi}. \quad (3.23)$$

Next, we calculate λ_1 from the problem (3.18) for v_2 . We integrate (3.18 a) over $0 < y < \infty$, and use $v_2''' \rightarrow 0$ as $y \rightarrow \infty$, to obtain that $\lambda_1 \int_0^\infty v_0^{-2} dy = 2\lambda_0 \int_0^\infty (v_1/v_0^3) dy$. Then, since $v_0 = 3y^2 + 1$, we get

$$\lambda_1 = \frac{8\sqrt{3}\lambda_0}{\pi} \int_0^\infty \frac{v_1}{(3y^2 + 1)^3} dy. \quad (3.24)$$

This integral can be directly evaluated by using (3.21) for v_1 . In this way, we obtain that

$$\lambda_1 \equiv \frac{8\sqrt{3}\lambda_0}{\pi} \left[-\frac{\lambda_0}{12\sqrt{3}} I_1 - \frac{\lambda_0}{36} I_2 + \frac{\lambda_0}{108} I_3 - \frac{\lambda_0}{12\sqrt{3}} I_4 \right], \quad (3.25)$$

where, upon repeated integration by parts, we calculate

$$\begin{aligned} I_1 &\equiv \int_0^\infty \frac{y^3 \tan^{-1}(\sqrt{3}y)}{(1+3y^2)^3} dy = \frac{1}{12} \int_0^\infty \left[\frac{2y \tan^{-1}(\sqrt{3}y)}{(1+3y^2)^2} + \frac{\sqrt{3}y^2}{(1+3y^2)^3} \right] dy \\ &= \frac{1}{12\sqrt{3}} \int_0^\infty \frac{dy}{(1+3y^2)^2} + \frac{1}{4\sqrt{3}} \int_0^\infty \frac{y^2 dy}{(1+3y^2)^3} = \frac{1}{12\sqrt{3}} \left(\frac{\pi}{4\sqrt{3}} \right) + \frac{1}{4\sqrt{3}} \left(\frac{\pi}{48\sqrt{3}} \right) = \frac{5\pi}{576}, \\ I_2 &\equiv \int_0^\infty \frac{y^2 dy}{(1+3y^2)^3} = \frac{\pi}{48\sqrt{3}}, \quad I_3 \equiv \int_0^\infty \frac{\log(1+3y^2)}{(1+3y^2)^3} dy = \frac{\pi(12 \log 2 - 7)}{32\sqrt{3}}, \\ I_4 &\equiv \int_0^\infty \frac{y \tan^{-1}(\sqrt{3}y)}{(1+3y^2)^3} dy = \frac{\sqrt{3}}{12} \int_0^\infty \frac{dy}{(1+3y^2)^3} = \frac{\sqrt{3}}{12} \left(\frac{\pi\sqrt{3}}{16} \right) = \frac{\pi}{64}. \end{aligned}$$

Upon substituting these results for I_j , for $j = 1, \dots, 4$, into (3.25), we obtain that

$$\lambda_1 = \frac{\lambda_0^2}{108} (3 \log 2 - 4) \approx -12.454. \quad (3.26)$$

Finally, we calculate b_1 from (3.18). We multiply (3.18 a) by v_0 and integrate the resulting expression to get

$$\int_0^R v_0 v_2'''' dy = 2\lambda_0 \int_0^R \frac{v_1}{v_0^2} dy - \lambda_1 \int_0^R \frac{1}{v_0} dy. \quad (3.27)$$

Since $v_1 \sim -2y^3$ and $v_0 \sim 3y^2$ as $y \rightarrow \infty$, then $v_1/v_0^2 \sim -2/(9y)$ as $y \rightarrow \infty$. Therefore, since the first integral on the right-hand side of (3.27) diverges as $R \rightarrow \infty$, we must re-write (3.27) as

$$\left[v_0 v_2'' \Big|_0^R - v_0' v_2'' \Big|_0 + \int_0^R v_0'' v_2'' dy \right] = 2\lambda_0 \int_0^R \left(\frac{v_1}{v_0^2} + \frac{2}{9(y+1)} \right) dy - \frac{4\lambda_0}{9} \log(R+1) - \lambda_1 \int_0^R \frac{1}{v_0} dy. \quad (3.28)$$

Then, by using $v_0 = 3y^2 + 1$ and the asymptotic behaviour of v_2 in (3.18 b), we take the limit $R \rightarrow \infty$ to get

$$\begin{aligned} \lim_{R \rightarrow \infty} \left[(3R^2 + 1) \frac{2\lambda_0}{27R^2} - 6R \left(2 - \frac{2\lambda_0}{27R} \right) + 6 \left(2R - \frac{2\lambda_0}{27} \log R - \frac{2\lambda_0}{27} + b_1 \right) + \frac{4\lambda_0}{9} \log(R+1) + \dots \right] \\ = 2\lambda_0 \int_0^\infty \left(\frac{v_1}{v_0^2} + \frac{2}{9(y+1)} \right) dy - \lambda_1 \int_0^\infty \frac{1}{v_0} dy \end{aligned} \quad (3.29)$$

Substituting $\int_0^\infty v_0^{-1} dy = \pi/(2\sqrt{3})$ together with (3.24) for λ_1 into (3.29), we calculate b_1 as

$$b_1 = -\frac{\lambda_0}{27} + \frac{\lambda_0}{3} \int_0^\infty \left(\frac{v_1}{v_0^2} + \frac{2}{9(y+1)} \right) dy - \frac{2\lambda_0}{3} \int_0^\infty \frac{v_1}{v_0^3} dy. \quad (3.30)$$

We summarize our asymptotic result as follows:

Principal Result 3.2: For $\varepsilon \equiv u(0) + 1 \rightarrow 0^+$, the maximal solution branch of (3.1) has asymptotic behaviour

$$\lambda_\varepsilon \sim \frac{48\sqrt{3}\varepsilon^{3/2}}{\pi} \left(1 + \frac{4\varepsilon^{1/2}}{3\sqrt{3}\pi} (3 \log 2 - 4) + \dots \right). \quad (3.31 a)$$

In the outer region, defined away from $x = 0$, a four-term expansion for u_ε is

$$u_\varepsilon = -1 + 3x^2 - 2x^3 + \varepsilon(1 - 2x + x^2) + \left(\varepsilon^{3/2} \log \varepsilon \right) u_{3/2} + \varepsilon^{3/2} u_1 + \dots. \quad (3.31 b)$$

Here $u_{3/2}$ is given in terms of $\lambda_0 = 48\sqrt{3}/\pi$ by (3.14 b), and u_1 is defined uniquely in terms of c_1 and b_1 of (3.23) and (3.30), respectively, by the boundary value problem (3.4 b) with singular behaviour (3.6).

A very favourable comparison of numerical and asymptotic results for $|u(0)|$ versus λ is shown in Fig. 8. The two-term approximation for λ in (3.31 a) is shown to be rather accurate even for λ not too small.

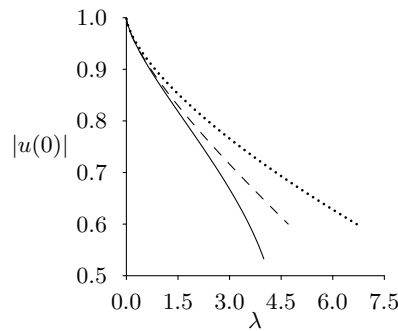


FIGURE 8. The full numerical result (solid line) for $|u(0)| = 1 - \varepsilon$ versus λ for the biharmonic problem (3.1) is compared with the one-term (dotted curve) and the two-term (dashed curve) asymptotic result given in (3.31 a).

A similar analysis can be done for the more general mixed biharmonic problem, formulated as

$$-u_{xxxx} + \beta u_{xx} = \frac{\tilde{\lambda}}{(1+u)^2}, \quad |x| < 1; \quad u(\pm 1) = u_x(\pm 1) = 0, \quad (3.32 a)$$

where we have defined β and $\tilde{\lambda}$ in terms of $\delta = \mathcal{O}(1)$ by

$$\beta = \delta^{-1}, \quad \lambda = \delta \tilde{\lambda}. \quad (3.32 b)$$

For a fixed $\delta = \mathcal{O}(1)$, we will construct the limiting behaviour of the maximal solution branch $u_\varepsilon, \tilde{\lambda}_\varepsilon$ in the limit $u_\varepsilon(0) + 1 = \varepsilon \rightarrow 0^+$. We will consider (3.32 a) on $0 \leq x < 1$ with symmetry conditions $u_x(0) = u_{xxx}(0) = 0$.

As for the pure biharmonic problem (3.1), the expansion for $\tilde{\lambda}_\varepsilon$ and the outer expansion for u_ε is (see (3.12)),

$$u_\varepsilon \sim u_0 + \varepsilon u_{1/2} + \varepsilon^{3/2} \log \varepsilon u_{3/2} + \varepsilon^{3/2} u_1 + \dots, \quad \tilde{\lambda}_\varepsilon \sim \varepsilon^{3/2} \tilde{\lambda}_0 + \varepsilon^2 \tilde{\lambda}_1 + \dots. \quad (3.33)$$

Upon substituting (3.33) into (3.32), and imposing the point constraints $u_0(0) = -1$ and $u_{0x}(0) = 0$, we obtain that

$$-u_{0xxxx} + \beta u_{0xx} = 0, \quad 0 < x < 1; \quad u_0(0) = -1, \quad u_{0x}(0) = 0, \quad u_0(1) = 0, \quad u_{0x}(1) = 0, \quad (3.34 a)$$

$$-u_{1xxxx} + \beta u_{1xx} = \frac{\tilde{\lambda}_0}{(1+u_0)^2}, \quad 0 < x < 1; \quad u_1(1) = 0, \quad u_{1x}(1) = 0. \quad (3.34 b)$$

Moreover, the two switchback terms $u_{1/2}$ and $u_{3/2}$ are taken to satisfy

$$-u_{1/2xxxx} + \beta u_{1/2xx} = 0, \quad 0 < x < 1; \quad u_{1/2}(0) = 1, \quad u_{1/2x}(0) = b_{1/2}, \quad u_{1/2}(1) = 0, \quad u_{1/2x}(1) = 0, \quad (3.35 a)$$

$$-u_{3/2xxxx} + \beta u_{3/2xx} = 0 \quad 0 < x < 1; \quad u_{3/2}(0) = c_{3/2}, \quad u_{3/2x}(0) = b_{3/2}, \quad u_{3/2}(1) = 0, \quad u_{3/2x}(1) = 0, \quad (3.35 b)$$

for some constants $c_{3/2}, b_{3/2}$, and $b_{1/2}$, to be found.

The solution to (3.34 a) for u_0 is given by

$$u_0(x) = -1 + C \left[\cosh(\sqrt{\beta}x) - 1 \right] + D \left[\sqrt{\beta}x - \sinh(\sqrt{\beta}x) \right], \quad (3.36 a)$$

where C and D are defined in terms of β by

$$C = \left[\sqrt{\beta} \coth\left(\frac{\sqrt{\beta}}{2}\right) - 2 \right]^{-1}, \quad D = \left[\sqrt{\beta} - 2 \tanh\left(\frac{\sqrt{\beta}}{2}\right) \right]^{-1}. \quad (3.36 b)$$

From (3.36), we calculate the local behaviour

$$u_0 \sim -1 + \alpha x^2 + \gamma x^3 + \frac{\alpha\beta}{12} x^4 + \dots, \quad \text{as } x \rightarrow 0, \quad (3.37 a)$$

where α and γ are given by

$$\alpha \equiv \frac{1}{2} u_{0xx}(0) = \left(\frac{\beta}{2}\right) \left[\sqrt{\beta} \coth\left(\frac{\sqrt{\beta}}{2}\right) - 2 \right]^{-1}, \quad \gamma \equiv \frac{1}{6} u_{0xxx}(0) = -\left(\frac{\beta^{3/2}}{6}\right) \left[\sqrt{\beta} - 2 \tanh\left(\frac{\sqrt{\beta}}{2}\right) \right]^{-1}. \quad (3.37 b)$$

As $\delta \rightarrow \infty$, corresponding to $\beta \rightarrow 0$, we obtain that $\alpha \rightarrow 3$ and $\gamma \rightarrow -2$, which agrees with the result for u_0 given in (3.5) for the pure biharmonic case. As required for the analysis below, we can readily show from (3.37 b) that $\alpha > 0$ and $\gamma < 0$ for all $\delta > 0$.

Next, from the problem (3.34 b) for u_1 , the local behaviour as $x \rightarrow 0$ for u_1 is

$$u_1 \sim \frac{\tilde{\lambda}_0}{6\alpha^2} \log x + \frac{\gamma\tilde{\lambda}_0}{\alpha^3} x \log x + c_1 + b_1 x, \quad \text{as } x \rightarrow 0, \quad (3.38)$$

where c_1 and b_1 , representing unknown coefficients associated with the homogeneous solution for u_1 , are to be determined. Next, we use the local behaviours (3.37 a) and (3.38) for u_0 and u_1 , respectively, together with the local behaviour for $u_{1/2}$ and $u_{3/2}$ from (3.35), to obtain the following near-field behaviour as $x \rightarrow 0$ of the outer expansion

in (3.33):

$$u \sim -1 + \alpha x^2 + \gamma x^3 + \frac{\alpha\beta}{12}x^4 + \cdots \varepsilon \left(1 + b_{1/2}x + u_{1/2xx}(0)\frac{x^2}{2} + \cdots \right) + \varepsilon^{3/2} \log \varepsilon (c_{3/2} + b_{3/2}x + \cdots) + \varepsilon^{3/2} \left(\frac{\tilde{\lambda}_0}{6\alpha^2} \log x + \frac{\gamma\tilde{\lambda}_0}{\alpha^3} x \log x + c_1 + b_1x + \cdots \right). \quad (3.39)$$

In terms in the inner variable y , defined by $x = \varepsilon^{1/2}y$, (3.39) becomes

$$u \sim -1 + \varepsilon (\alpha y^2 + 1) + (\varepsilon^{3/2} \log \varepsilon) \left(c_{3/2} + \frac{\tilde{\lambda}_0}{12\alpha^2} \right) + \varepsilon^{3/2} \left(\gamma y^3 + b_{1/2}y + \frac{\tilde{\lambda}_0}{6\alpha^2} \log y + c_1 \right) + (\varepsilon^2 \log \varepsilon) \left(b_{3/2}y + \frac{\gamma\tilde{\lambda}_0}{2\alpha^3}y \right) + \varepsilon^2 \left(u_{1/2xx}(0)\frac{y^2}{2} + \frac{\gamma\tilde{\lambda}_0}{\alpha^3}y \log y + \frac{\alpha\beta}{12}y^4 + b_1y \right) + \cdots. \quad (3.40)$$

To eliminate the $\mathcal{O}(\varepsilon^{3/2} \log \varepsilon)$ and $\mathcal{O}(\varepsilon^2 \log \varepsilon)$ terms, which cannot be matched by the inner solution, we must choose

$$c_{3/2} = -\frac{\tilde{\lambda}_0}{12\alpha^2}, \quad b_{3/2} = -\frac{\gamma\tilde{\lambda}_0}{2\alpha^3}. \quad (3.41)$$

With $c_{3/2}$ and $b_{3/2}$ given by (3.41), we can then calculate the solution $u_{3/2}$ to (3.35 *b*) explicitly.

In the inner region, we let $y = x/\varepsilon^{1/2}$ and $v(y) = u(\varepsilon^{1/2}y)$, and we expand v as in (3.16). Then, from (3.32) and (3.33) for $\tilde{\lambda}_\varepsilon$, we obtain that the leading-order inner solution is $v_0 = \alpha y^2 + 1$, and that v_1 satisfies

$$v_1'''' = -\frac{\tilde{\lambda}_0}{v_0^2}, \quad 0 < y < \infty; \quad v_1(0) = v_1'(0) = v_1'''(0) = 0, \quad (3.42 a)$$

$$v_1 \sim \gamma y^3 + b_{1/2}y + \frac{\tilde{\lambda}_0}{6\alpha^2} \log y + c_1, \quad \text{as } y \rightarrow \infty, \quad (3.42 b)$$

while v_2 is the solution of

$$v_2'''' = \frac{2\tilde{\lambda}_0}{v_0^3}v_1 - \frac{\tilde{\lambda}_1}{v_0^2} + \beta v_0'', \quad 0 < y < \infty; \quad v_2(0) = v_2'(0) = v_2'''(0) = 0, \quad (3.43 a)$$

$$v_2 \sim \frac{\alpha\beta}{12}y^4 + u_{1/2xx}(0)\frac{y^2}{2} + \frac{\gamma\tilde{\lambda}_0}{\alpha^3}y \log y + b_1y + \cdots, \quad \text{as } y \rightarrow \infty. \quad (3.43 b)$$

By repeating the analysis of the pure biharmonic case in (3.19)–(3.30), we can determine $\tilde{\lambda}_0$, $\tilde{\lambda}_1$, $b_{1/2}$, c_1 , and b_1 , from (3.42) and (3.43). We remark that in determining $\tilde{\lambda}_1$ and b_1 from (3.43), we first must write $v_2 = \tilde{v}_2 + \alpha\beta y^4/12$, and obtain a problem for \tilde{v}_2 without the $\beta v_0'' = 2\alpha\beta$ term in (3.43 *a*). From the problem (3.42) for v_1 , we calculate

$$\tilde{\lambda}_0 = -\frac{24\gamma\sqrt{\alpha}}{\pi}, \quad b_{1/2} = \frac{3\gamma}{\alpha} = -\sqrt{\beta} \coth\left(\frac{\sqrt{\beta}}{2}\right), \quad c_1 = \frac{\tilde{\lambda}_0}{\alpha^2} \left(\frac{2}{9} + \frac{\log \alpha}{12} \right). \quad (3.44)$$

By using a simple scaling relation to transform (3.42) to (3.17), with solution (3.21), the solution to (3.42) for v_1 is

$$v_1 = -\frac{\tilde{\lambda}_0}{12\sqrt{\alpha}}y^3 \tan^{-1}(\sqrt{\alpha}y) - \frac{\tilde{\lambda}_0}{12\alpha}y^2 + \frac{\tilde{\lambda}_0}{12\alpha^2} \log(1 + \alpha y^2) - \frac{\tilde{\lambda}_0}{4\alpha^{3/2}}y \tan^{-1}(\sqrt{\alpha}y). \quad (3.45)$$

In terms of v_1 , we calculate from the problem (3.43) for v_2 that

$$\tilde{\lambda}_1 = \frac{8\tilde{\lambda}_0\sqrt{\alpha}}{\pi} \int_0^\infty \frac{v_1}{v_0^3} dy, \quad b_1 = \frac{\tilde{\lambda}_0\gamma}{2\alpha^3} + \frac{\tilde{\lambda}_0}{\alpha} \int_0^\infty \left(\frac{v_1}{v_0^2} - \frac{\gamma}{\alpha^2(y+1)} \right) dy - \frac{2\tilde{\lambda}_0}{\alpha} \int_0^\infty \frac{v_1}{v_0^3} dy, \quad (3.46)$$

where $v_0 = \alpha y^2 + 1$. The integral term in λ_1 above can be evaluated explicitly as was done for the pure biharmonic

case in (3.25)-(3.26)). The exact expression is $\bar{\lambda}_1 = \lambda_0^2 (3 \log 2 - 4) / (12\alpha^2)$. We summarize our result for (3.32) as follows:

Principal Result 3.3: For $\varepsilon \equiv u(0) + 1 \rightarrow 0^+$, the maximal solution branch of (3.32) has the asymptotic behaviour

$$\tilde{\lambda}_\varepsilon \sim -\frac{24\gamma\sqrt{\alpha}\varepsilon^{3/2}}{\pi} \left(1 - \frac{2\gamma\varepsilon^{1/2}}{\alpha^{3/2}\pi} (3 \log 2 - 4) + \dots \right), \quad (3.47 a)$$

where α and γ are defined in terms of $\beta = \delta^{-1}$ by (3.37 b). In the outer region, defined away from $x = 0$, a four-term expansion for u_ε is

$$u_\varepsilon \sim u_0 + \varepsilon u_{1/2} + \varepsilon^{3/2} \log \varepsilon u_{3/2} + \varepsilon^{3/2} u_1 + \dots \quad (3.47 b)$$

Here u_0 is given explicitly in (3.36), while $u_{1/2}$ and $u_{3/2}$ are the solutions of (3.35) in terms of the coefficients $c_{3/2}$ and $b_{3/2}$, defined in (3.41), and the coefficient $b_{1/2}$ given in (3.44). Finally, u_1 satisfies (3.34 b), subject to the local behaviour (3.38), where c_1 and b_1 are defined in (3.44) and (3.46), respectively.

We conclude this section with a few remarks. First, we note that since $\alpha > 0$ and $\gamma < 0$ for all $\delta > 0$, the limiting behaviour in (3.47 a) satisfies $\tilde{\lambda}_\varepsilon > 0$, and is defined for all $\delta > 0$. For $\delta \rightarrow \infty$, for which $\alpha \rightarrow 3$ and $\gamma \rightarrow -2$, (3.47 a) agrees with the result in (3.31 a) for the pure biharmonic problem. Alternatively, for $0 < \delta \ll 1$, we calculate from (3.37 b) that $\alpha \sim [2\sqrt{\delta}]^{-1}$ and $\gamma \sim -[6\delta]^{-1}$. The expansion for $\tilde{\lambda}_\varepsilon$ in (3.47 a) is not uniformly valid as $\delta \rightarrow 0$ when the second term in (3.47 a) is comparable to the first term. This occurs when $\varepsilon^{1/2}\gamma/\alpha^{3/2} = \mathcal{O}(1)$. Using $\alpha = \mathcal{O}(\delta^{-1/2})$ and $\gamma = \mathcal{O}(\delta^{-1})$, we obtain that $\varepsilon^{1/2}\gamma/\alpha^{3/2} = \mathcal{O}(1)$ when $\delta = \mathcal{O}(\varepsilon^2)$. Hence, (3.47 a) holds only when $\delta \gg \mathcal{O}(\varepsilon^2)$. Finally, we remark that the two switchback terms can be written explicitly in the form $u_{1/2}(x) = w(x; 1, b_{1/2})$ and $u_{3/2}(x) = w(x; c_{3/2}, b_{3/2})$, where $w(x; w_0, w_1)$ is the solution to $-w_{xxxx} + \beta w_{xx} = 0$ with $w(0) = w_0$, $w_x(0) = w_1$, $w(1) = w_x(1) = 0$, which is given explicitly by

$$w(x) = w_0 + w_1 x + \mathcal{C} \left[\cosh(\sqrt{\beta}x) - 1 \right] + \mathcal{D} \left[\sqrt{\beta}x - \sinh(\sqrt{\beta}x) \right], \quad (3.48 a)$$

where \mathcal{C} and \mathcal{D} is the unique solution to the 2×2 linear algebraic system

$$\mathcal{C} \left[\cosh(\sqrt{\beta}) - 1 \right] + \mathcal{D} \left[\sqrt{\beta} - \sinh(\sqrt{\beta}) \right] = -(w_0 + w_1), \quad (3.48 b)$$

$$\mathcal{C}\sqrt{\beta} \sinh(\sqrt{\beta}) + \mathcal{D}\sqrt{\beta} \left[1 - \cosh(\sqrt{\beta}) \right] = -w_1. \quad (3.48 c)$$

In Fig. 9 we show a favourable comparison between the two-term asymptotic result (3.47 a) and the full numerical result for $\lambda_\varepsilon = \delta \tilde{\lambda}_\varepsilon$ when $\delta = 0.1$ and $\delta = 1.0$. We observe that the two-term asymptotic result agrees remarkably well with the full numerical result even when ε is only moderately small.

4 Asymptotics of Maximal Solution Branch as $\lambda \rightarrow 0$ for the Biharmonic Problem: Unit Disk

In the unit disk in \mathbb{R}^2 , we now construct the limiting asymptotic behaviour of the maximal solution branch of the pure biharmonic nonlinear eigenvalue problem

$$\Delta^2 u = -\frac{\lambda}{(1+u)^2}, \quad 0 < r < 1; \quad u(1) = u_r(1) = 0, \quad (4.1)$$

where $\Delta u \equiv u_{rr} + r^{-1}u_r$. For $\delta > 0$, we will also consider the mixed biharmonic problem

$$\delta \Delta^2 u - \Delta u = -\frac{\lambda}{(1+u)^2}, \quad 0 < r < 1; \quad u(1) = u_r(1) = 0, \quad (4.2)$$

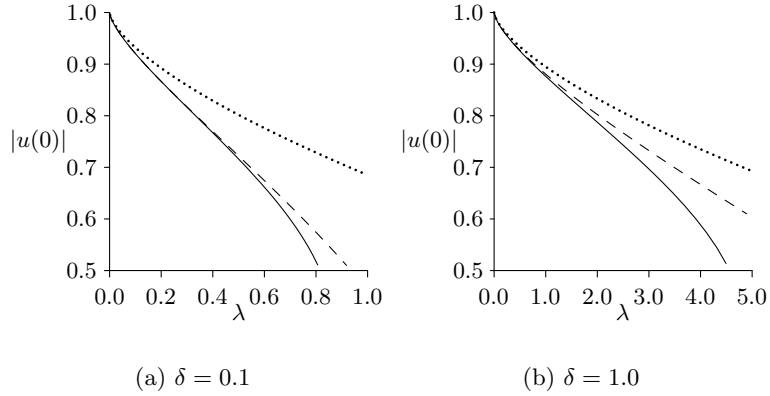


FIGURE 9. The full numerical result (solid line) for $|u(0)| = 1 - \varepsilon$ versus λ for the mixed biharmonic problem (3.32) is compared with the one-term (dotted curve) and the two-term (dashed curve) asymptotic result given in (3.47 a). Left figure: $\delta = 0.1$. Right figure: $\delta = 1.0$.

In each case, we set $u(0) + 1 = \varepsilon$ and construct a solution u_ε , λ_ε such that $\lambda_\varepsilon \sim \nu(\varepsilon) \lambda_0$ as $\varepsilon \rightarrow 0^+$, where $\nu(\varepsilon) \ll 1$ is a gauge function to be determined. One of the main challenges in constructing the asymptotic solution of (4.1) as $u(0) \rightarrow -1^+$ is determining $\nu(\varepsilon)$ and the correct expansion of u . This is achieved by matching an inner solution valid in a small neighbourhood of the origin to an outer expansion valid elsewhere. Since the analysis for (4.1) and (4.2) is very similar, we will only provide a full analysis for the pure biharmonic case, and simply state the main results for the mixed problem.

We first pose naive expansions for λ and the outer solution in the form

$$u = u_0 + \nu(\varepsilon) u_1 + \dots, \quad \lambda_\varepsilon = \nu(\varepsilon) \lambda_0 + \dots. \quad (4.3)$$

Upon substituting (4.3) into (4.1), we obtain on $0 < r < 1$ that u_0 and u_1 satisfy

$$\Delta^2 u_0 = 0, \quad u_0(1) = u_{0r}(1) = 0; \quad \Delta^2 u_1 = -\frac{\lambda_0}{(1 + u_0)^2}, \quad u_1(1) = u_{1r}(1) = 0. \quad (4.4)$$

By imposing the point constraints $u_0(0) = -1$ and $u_{0r}(0) = 0$, the solution to (4.4) for u_0 is

$$u_0 = -1 + r^2 - 2r^2 \log r, \quad (4.5)$$

while u_1 satisfies

$$\Delta^2 u_1 = -\frac{\lambda_0}{r^4(1 - 2 \log r)^2}, \quad 0 < r < 1; \quad u_1(1) = u_1'(1) = 0. \quad (4.6)$$

Note that $u_{0r}(0) = 0$, while $u_{0rr}(r)$ diverges as $r \rightarrow 0$. This shows that we need a boundary layer near $r = 0$ in order to satisfy the required symmetry condition $u_{rrr}(0) = 0$.

To determine the behaviour of u_1 as $r \rightarrow 0$, we introduce the new variables $\eta = -\log r$ and $w(\eta) = u(e^{-\eta})$, so that $\eta \rightarrow \infty$ as $r \rightarrow 0$. From (4.6), we get that $w(\eta)$ satisfies

$$w'''' + 4w''' + 4w'' = -\frac{\lambda_0}{(1 + 2\eta)^2} = -\frac{\lambda_0}{4\eta^2} \left(1 + \frac{1}{2\eta}\right)^{-2}. \quad (4.7)$$

By using $(1 + h)^{-2} \sim 1 - 2h + 3h^2 + \dots$, for $h \ll 1$, we readily calculate from (4.7) that

$$w \sim \frac{\lambda_0}{16} \log \eta - \frac{\lambda_0}{32\eta} - \frac{3\lambda_0}{128\eta^2} - \frac{13\lambda_0}{384\eta^3} + \dots, \quad \text{as } \eta \rightarrow \infty.$$

Therefore, upon setting $\eta = -\log r$, we obtain that u_1 has the near-field asymptotic behaviour

$$u_1 \sim \frac{\lambda_0}{16} \log(-\log r) + \frac{\lambda_0}{32 \log r} - \frac{3\lambda_0}{128 \log^2 r} + \frac{13\lambda_0}{384 \log^3 r} + a_1 + a_2 \log r + \dots, \quad \text{as } r \rightarrow 0, \quad (4.8)$$

where a_1 and a_2 are constants related to the solution of the homogeneous problem for u_1 . By determining these constants below, and then by satisfying the two boundary conditions $u_1(1) = u_{1r}(1) = 0$, the solution u_1 to (4.6) can be found uniquely. For $r \rightarrow 0$, the two-term outer expansion for u , given by (4.3), has the limiting behaviour

$$u \sim -1 + r^2 - 2r^2 \log r + \nu \left(\frac{\lambda_0}{16} \log(-\log r) + \frac{\lambda_0}{32 \log r} - \frac{3\lambda_0}{128 \log^2 r} + \frac{13\lambda_0}{384 \log^3 r} + a_1 + a_2 \log r \right) + \dots. \quad (4.9)$$

In the inner region for (4.1) near the origin, we introduce the inner variables v and ρ defined by

$$u = -1 + \varepsilon v(\rho), \quad \rho = r/\gamma, \quad (4.10)$$

where $\gamma \ll 1$ is the boundary layer width to be found. Upon setting $r = \gamma \rho$ in (4.9), we obtain

$$u = -1 + \gamma^2 \rho^2 - 2\gamma^2 \rho^2 (\log \gamma + \log \rho) + \mathcal{O}[\nu \log(-\log \gamma)], \quad (4.11)$$

for $\gamma \ll 1$. The largest term in (4.11) must be $\mathcal{O}(\varepsilon)$ if the outer and inner expansions are to be successfully matched. In addition, since $u_{0rr}(0)$ is infinite, we expect that $u_{rr}(0) = (\varepsilon/\gamma^2)v''(0)$ is not finite as $\varepsilon \rightarrow 0^+$. These considerations show that the boundary layer width is determined implicitly in terms of ε by

$$-\gamma^2 \log \gamma = \frac{\gamma^2}{\sigma} = \varepsilon, \quad \text{and} \quad \sigma \equiv -\frac{1}{\log \gamma}, \quad (4.12)$$

Next, we write (4.9) in terms of ρ , ε , and σ , as

$$u \sim -1 + 2\rho^2 \varepsilon + \sigma \varepsilon (-2\rho^2 \log \rho + \rho^2) + \nu \left(-\frac{\lambda_0}{16} \log \sigma + \frac{\lambda_0}{16} \log(1 - \sigma \log \rho) - \frac{\lambda_0}{32} \frac{\sigma}{(1 - \sigma \log \rho)} - \frac{3\lambda_0 \sigma^2}{128(1 - \sigma \log \rho)^2} - \frac{13\lambda_0 \sigma^3}{384(1 - \sigma \log \rho)^3} + a_1 - \frac{a_2}{\sigma} + a_2 \log \rho \right) + \dots. \quad (4.13)$$

Expanding terms in (4.13) for $\sigma \ll 1$, and collecting terms at each order, we obtain that

$$u \sim -1 + \varepsilon \left[2\rho^2 + \sigma(-2\rho^2 \log \rho + \rho^2) + \frac{\nu}{\varepsilon} \left[-\frac{\lambda_0}{16} \log \sigma + a_1 - \frac{a_2}{\sigma} + a_2 \log \rho + \sigma \left(-\frac{\lambda_0}{16} \log \rho - \frac{\lambda_0}{32} \right) + \sigma^2 \left(-\frac{\lambda_0}{32} \log^2 \rho - \frac{\lambda_0}{32} \log \rho - \frac{3\lambda_0}{128} \right) + \sigma^3 \left(-\frac{\lambda_0}{48} \log^3 \rho - \frac{\lambda_0}{32} \log^2 \rho - \frac{3\lambda_0}{64} \log \rho - \frac{13\lambda_0}{384} \right) + \dots \right] \right]. \quad (4.14)$$

To determine the scaling of ν , we first substitute the local variables (4.10) into (4.1) to obtain the inner problem

$$\Delta_\rho^2 v = -\frac{\sigma^2 \nu [\lambda_0 + \dots]}{\varepsilon v^2}, \quad 0 < \rho < \infty; \quad v(0) = 1, \quad v'(0) = v'''(0) = 0, \quad (4.15)$$

where Δ_ρ^2 is the biharmonic operator in terms of ρ . The largest term in (4.14) is $\mathcal{O}(\varepsilon)$, which suggests that we expand v as $v = v_0 + \sigma v_1 + \mathcal{O}(\sigma^2)$. Therefore, the only feasible scalings for ν are $\nu = \varepsilon \sigma^{-2}$ or $\nu = \varepsilon \sigma^{-1}$. If we choose $\nu = \varepsilon \sigma^{-2}$, then $\Delta_\rho^2 v_0 = -\lambda_0/v_0^2$ with $v_0 \sim 2\rho^2$ as $\rho \rightarrow \infty$, which has no solution. Therefore, we must choose

$$\nu = \frac{\varepsilon}{\sigma} = -\gamma^2 \log \gamma \left(\frac{-1}{\log \gamma} \right)^{-1} = \gamma^2 (\log \gamma)^2. \quad (4.16)$$

Substituting (4.16) for ν into (4.14), and recalling $u = -1 + \varepsilon v$, we obtain from the matching condition that the

asymptotic expansion of the solution v to (4.15) must have the following far-field behaviour as $\rho \rightarrow \infty$:

$$\begin{aligned} v \sim & -\frac{1}{\sigma^2} a_2 - \frac{\log \sigma}{\sigma} \frac{\lambda_0}{16} + \frac{1}{\sigma} (a_1 + a_2 \log \rho) + \left(2\rho^2 - \frac{\lambda_0}{16} \log \rho - \frac{\lambda_0}{32} \right) \\ & + \sigma \left(-2\rho^2 \log \rho + \rho^2 - \frac{\lambda_0}{32} \log^2 \rho - \frac{\lambda_0}{32} \log \rho - \frac{3\lambda_0}{128} \right) + \sigma^2 \left(-\frac{\lambda_0}{48} \log^3 \rho - \frac{\lambda_0}{32} \log^2 \rho - \frac{3\lambda_0}{64} \log \rho - \frac{13\lambda_0}{384} \right) + \dots \end{aligned} \quad (4.17)$$

Since we will expand (4.15) with $v = v_0 + \sigma v_1 + \mathcal{O}(\sigma^2)$, the $\mathcal{O}(\sigma^{-2})$, $\mathcal{O}(\sigma^{-1})$, and $\mathcal{O}(\sigma^{-1} \log \sigma)$, terms in (4.17) are too large, and they can only be removed by adjusting the outer expansion by introducing switchback terms. The modified outer and nonlinear eigenvalue expansions, in place of the naive original expansions (4.3), is

$$u = u_0 + \frac{\varepsilon \log \sigma}{\sigma} u_{1/2} + \frac{\varepsilon}{\sigma} u_1 + \varepsilon \log \sigma u_{3/2} + \varepsilon u_2 + \varepsilon \sigma \log \sigma u_{5/2} + \varepsilon \sigma u_3 + \varepsilon \sigma^2 \log \sigma u_{7/2} + \varepsilon \sigma^2 u_4 + \dots, \quad (4.18 a)$$

$$\lambda = \frac{\varepsilon}{\sigma} [\lambda_0 + \sigma \lambda_1 + \sigma^2 \lambda_2 + \sigma^3 \lambda_3 + \dots]. \quad (4.18 b)$$

Such a lengthy expansion is required in order to completely specify the inner solution $v(\rho)$ up to terms of order $\mathcal{O}(\sigma)$. Upon substituting (4.18) into (4.1), we obtain for $j = 1, \dots, 4$ that on $0 < r < 1$ the switchback terms satisfy

$$\Delta^2 u_{(2j-1)/2} = 0; \quad u_{(2j-1)/2}(0) = f_{(2j-1)/2}, \quad \partial_r u_{(2j-1)/2}(0) = 0, \quad u_{(2j-1)/2}(1) = \partial_r u_{(2j-1)/2}(1) = 0, \quad (4.19)$$

which has the solution

$$u_{(2j-1)/2}(r) = f_{(2j-1)/2} (1 - r^2 + 2r^2 \log r), \quad j = 1, \dots, 4, \quad (4.20)$$

where $f_{(2j-1)/2}$ for $j = 1, \dots, 4$ are constants to be determined. Moreover, for $j = 2, 3, 4$, $u_j(r)$ satisfies

$$\Delta^2 u_j = -\frac{\lambda_{j-1}}{(1+u_0)^2}, \quad 0 < r < 1; \quad u_j(1) = \partial_r u_j(1) = 0, \quad j = 2, 3, 4. \quad (4.21)$$

The asymptotic behaviour of the solution for u_j as $r \rightarrow 0$ for $j = 2, 3, 4$ is (see equation (4.8)),

$$\begin{pmatrix} u_2 \\ u_3 \\ u_4 \end{pmatrix} \sim \begin{pmatrix} \lambda_1 \\ \lambda_2 \\ \lambda_3 \end{pmatrix} \left(\frac{\log(-\log r)}{16} + \frac{1}{32 \log r} - \frac{3}{128 \log^2 r} + \frac{13}{384 \log^3 r} \right) + \begin{pmatrix} b_1 \\ c_1 \\ d_1 \end{pmatrix} + \begin{pmatrix} b_2 \\ c_2 \\ d_2 \end{pmatrix} \log r + \dots \quad (4.22)$$

Here b_1, b_2, c_1, c_2, d_1 , and d_2 , are constants pertaining to the homogeneous solution. These constants are fixed in the matching process below, which then determines u_j for $j = 2, 3, 4$ uniquely.

From (4.18), (4.20), and (4.22), together with $u = -1 + \varepsilon v$, the matching condition between the outer and inner solutions leads to the following far-field behaviour for the inner solution v as $\rho \rightarrow \infty$:

$$\begin{aligned} v \sim & -\frac{1}{\sigma^2} a_2 + \frac{\log \sigma}{\sigma} \left(f_{1/2} - \frac{\lambda_0}{16} \right) + \log \sigma \left(f_{3/2} - \frac{\lambda_1}{16} \right) + \sigma \log \sigma \left(f_{5/2} - \frac{\lambda_2}{16} \right) + \sigma^2 \log \sigma \left(f_{7/2} - \frac{\lambda_3}{16} \right) \\ & + \frac{1}{\sigma} (a_1 - b_2 + a_2 \log \rho) + \left(b_1 - \frac{\lambda_0}{32} + c_2 + 2\rho^2 + \left(b_2 - \frac{\lambda_0}{16} \right) \log \rho \right) \\ & + \sigma \left(-2\rho^2 \log \rho + \rho^2 - \frac{\lambda_0}{32} \log^2 \rho + \left(c_2 - \frac{\lambda_0}{32} - \frac{\lambda_1}{16} \right) \log \rho + c_1 - d_2 - \frac{\lambda_1}{32} - \frac{3\lambda_0}{128} \right) \\ & + \sigma^2 \left(-\frac{\lambda_0}{48} \log^3 \rho - \left(\frac{\lambda_1}{32} + \frac{\lambda_0}{32} \right) \log^2 \rho + \left(d_2 - \frac{\lambda_2}{16} - \frac{\lambda_1}{32} - \frac{3\lambda_0}{64} \right) \log \rho + d_1 - e_2 - \frac{\lambda_2}{32} - \frac{3\lambda_1}{128} - \frac{13\lambda_0}{384} \right) \\ & + \mathcal{O}(\sigma^3). \end{aligned} \quad (4.23)$$

The constant e_2 in the order $\mathcal{O}(\sigma^2)$ term above arises from the homogeneous component to the solution u_5 of the $\varepsilon \sigma^3 u_5$ term in the outer expansion, not explicitly written in (4.18 a).

Since the expansion of the inner solution $v(\rho)$ is

$$v = v_0 + \sigma v_1 + \sigma^2 v_2 + \dots, \quad (4.24)$$

the constant terms in (4.23), which are larger than $\mathcal{O}(1)$, and the $\mathcal{O}(\sigma^p \log \sigma)$ terms in (4.23), must all be eliminated. In this way, we obtain that

$$a_1 = b_2, \quad a_2 = 0; \quad f_{(2j-1)/2} = \frac{\lambda_{j-1}}{16}, \quad j = 1, \dots, 4, \quad (4.25)$$

so that (4.23) becomes

$$\begin{aligned} v \sim & \left[b_1 - \frac{\lambda_0}{32} + c_2 + 2\rho^2 + \left(b_2 - \frac{\lambda_0}{16} \right) \log \rho \right] \\ & + \sigma \left[-2\rho^2 \log \rho + \rho^2 - \frac{\lambda_0}{32} \log^2 \rho + \left(c_2 - \frac{\lambda_0}{32} - \frac{\lambda_1}{16} \right) \log \rho + c_1 - d_2 - \frac{\lambda_1}{32} - \frac{3\lambda_0}{128} \right] \\ & + \sigma^2 \left[-\frac{\lambda_0}{48} \log^3 \rho - \left(\frac{\lambda_1}{32} + \frac{\lambda_0}{32} \right) \log^2 \rho + \left(d_2 - \frac{\lambda_2}{16} - \frac{\lambda_1}{32} - \frac{3\lambda_0}{64} \right) \log \rho + d_1 - e_2 - \frac{\lambda_2}{32} - \frac{3\lambda_1}{128} - \frac{13\lambda_0}{384} \right] \\ & + \mathcal{O}(\sigma^3) \end{aligned} \quad (4.26)$$

From (4.24), (4.15), and (4.26), we obtain that v_0 satisfies

$$\Delta_\rho^2 v_0 = 0, \quad 0 < \rho < \infty; \quad v_0(0) = 1, \quad v_0'(0) = v_0'''(0) = 0; \quad v_0 \sim 2\rho^2, \quad \text{as } \rho \rightarrow \infty. \quad (4.27)$$

The solution is $v_0 = 2\rho^2 + 1$. Then, from the first line in (4.26) we determine the constants b_1 and b_2 as

$$b_2 = \frac{\lambda_0}{16}, \quad b_1 = 1 + \frac{\lambda_0}{32} + c_2. \quad (4.28)$$

From the $\mathcal{O}(\sigma)$ terms in (4.15), (4.24), and (4.26), we obtain that v_1 satisfies

$$\Delta_\rho^2 v_1 = -\frac{\lambda_0}{v_0^2} \quad 0 < \rho < \infty; \quad v_1(0) = v_1'(0) = v_1'''(0) = 0, \quad (4.29 a)$$

with the far-field behaviour

$$v_1 \sim -2\rho^2 \log \rho + \rho^2 - \frac{\lambda_0}{32} \log^2 \rho + \chi_1 \log \rho + \chi_2, \quad \text{as } \rho \rightarrow \infty. \quad (4.29 b)$$

Here we have defined χ_1 and χ_2 by

$$\chi_1 \equiv c_2 - \frac{\lambda_0}{32} - \frac{\lambda_1}{16}, \quad \chi_2 \equiv c_1 - d_2 - \frac{\lambda_1}{32} - \frac{3\lambda_0}{128}. \quad (4.29 c)$$

From the $\mathcal{O}(\sigma^2)$ terms in (4.15), (4.24), and (4.26), we obtain that v_2 satisfies

$$\Delta_\rho^2 v_2 = -\frac{\lambda_1}{v_0^2} + \frac{2\lambda_0}{v_0^3} v_1, \quad 0 < \rho < \infty; \quad v_2(0) = v_2'(0) = v_2'''(0) = 0, \quad (4.30 a)$$

with the following far-field behaviour as $\rho \rightarrow \infty$:

$$v_2 \sim -\frac{\lambda_0}{48} \log^3 \rho - \left(\frac{\lambda_1}{32} + \frac{\lambda_0}{32} \right) \log^2 \rho + \left(d_2 - \frac{\lambda_2}{16} - \frac{\lambda_1}{32} - \frac{3\lambda_0}{64} \right) \log \rho + d_1 - e_2 - \frac{\lambda_2}{32} - \frac{3\lambda_1}{128} - \frac{13\lambda_0}{384} + \dots \quad (4.30 b)$$

The problem (4.29) determines the constants λ_0 , χ_1 , and χ_2 . Thus, (4.29 c) fixes c_2 in terms of λ_0 and λ_1 , and (4.28) determines b_1 . However, (4.29 c) only provides one of the two required equations to determine c_1 . As shown below, the additional equation is provided by the problem (4.30) for v_2 . To determine λ_0 , we apply the divergence

theorem to (4.29 a) to get

$$\lim_{R \rightarrow \infty} \left[\int_0^R \left(\Delta_\rho^2 v_1 + \frac{\lambda_0}{(1+2\rho^2)^2} \right) \rho d\rho \right] = \lim_{R \rightarrow \infty} \left[\rho \frac{d}{d\rho} (\Delta_\rho v_1) \Big|_{\rho=R} + \frac{\lambda_0}{4} \right] = 0. \quad (4.31)$$

We then use the leading-order term in the far-field behaviour (4.29 b) to obtain $\Delta_\rho v_1 \sim -8 \log \rho$ as $\rho \rightarrow \infty$. Therefore, (4.31) yields $\lambda_0 = 32$, so that $a_1 = 2$ and $b_2 = 2$, from (4.25) and (4.28), respectively. We remark that λ_0 is determined solely by the leading-order behaviour $v_1 \sim -2\rho^2 \log \rho$, while the correction term ρ^2 in (4.29 b) specifies v_1 uniquely, and allows for the determination of χ_1 and χ_2 in (4.29 b) as we now show.

To determine χ_1 and χ_2 , we first integrate (4.29 a) to obtain

$$\Delta_\rho v_1 = -4 \log(1+2\rho^2) + C, \quad (4.32)$$

with the value $C = 4(\log 2 - 1)$ obtained by using the far-field behaviour (4.29 b) in (4.32). Next, by integrating (4.32) with $v_1'(0) = 0$, we obtain the ODE initial value problem

$$v_{1\rho} = -2\rho \log(\rho^2 + 1/2) - \rho^{-1} \log(1+2\rho^2), \quad v_1(0) = 0. \quad (4.33)$$

A further integration of (4.33) yields

$$v_1 = \rho^2 - \frac{1}{2} \log 2 - \left(\rho^2 + \frac{1}{2} \right) \log \left(\rho^2 + \frac{1}{2} \right) - \int_0^\rho \frac{\log(1+2y^2)}{y} dy. \quad (4.34)$$

In order to identify the constants χ_1 and χ_2 in (4.29 b), we must determine the asymptotic expansion of (4.34) as $\rho \rightarrow \infty$. To do so, we must calculate the divergent integral in (4.34), by re-writing it as

$$\begin{aligned} I &\equiv \int_0^\rho \frac{\log(1+2y^2)}{y} dy = \frac{1}{2} \int_0^{2\rho^2} \frac{\log(1+x)}{x} dx = \frac{1}{2} \left[\int_0^1 \frac{\log(1+x)}{x} dx + \int_1^{2\rho^2} \frac{\log(1+x)}{x} dx \right], \\ &= \frac{\pi^2}{24} + \frac{1}{2} \int_1^{2\rho^2} \frac{\log(1+x)}{x} dx = \frac{\pi^2}{24} + \frac{1}{2} \left[\int_1^{2\rho^2} \left(\frac{\log(1+x)}{x} - \frac{\log x}{x} \right) dx + \int_1^{2\rho^2} \frac{\log x}{x} dx \right], \\ &= \frac{\pi^2}{24} + \frac{1}{4} [\log(2\rho^2)]^2 + \frac{1}{2} \int_1^{2\rho^2} \frac{\log(1+1/x)}{x} dx, \end{aligned}$$

where we have used $\int_0^1 x^{-1} \log(1+x) dx = \pi^2/12$. Therefore, (4.34) becomes

$$v_1 = -(\rho^2 + 1/2) \log(\rho^2 + 1/2) + \rho^2 - \frac{1}{2} \log 2 - \frac{\pi^2}{24} - \log^2 \rho - \log 2 \log \rho - \frac{1}{4} \log^2 2 - \frac{1}{2} \int_1^{2\rho^2} \frac{\log(1+1/x)}{x} dx, \quad (4.35)$$

where the integral term in (4.35) is finite as $\rho \rightarrow \infty$. Therefore, for $\rho \rightarrow \infty$, we obtain

$$v_1 = -2\rho^2 \log \rho + \rho^2 - \log^2 \rho - (1 + \log 2) \log \rho - \left(\frac{1}{2} + \frac{1}{2} \log 2 + \frac{1}{4} \log^2 2 + \frac{\pi^2}{24} + \frac{1}{2} \int_1^\infty \frac{\log(1+1/x)}{x} dx \right) + o(1),$$

where $\int_1^\infty x^{-1} \log(1+x^{-1}) dx = \int_0^1 u^{-1} \log(1+u) du = \pi^2/12$. Upon comparing this asymptotic result with (4.29 b), we identify χ_1 and χ_2 as

$$\chi_1 = -1 - \log 2, \quad \chi_2 = -\frac{1}{2} - \frac{1}{2} \log 2 - \frac{\pi^2}{12} - \frac{1}{4} \log^2 2. \quad (4.36)$$

Therefore, from (4.29 c) and (4.28), we obtain that

$$c_2 = \frac{\lambda_0}{32} + \frac{\lambda_1}{16} - 1 - \log 2, \quad b_1 = \frac{1}{16} (\lambda_0 + \lambda_1) - \log 2. \quad (4.37)$$

By proceeding to the next order problem (4.30) for v_2 we will determine λ_1 and obtain additional equations

relating the unknown constants d_1 , d_2 , and e_2 . The value of λ_1 is obtained by multiplying (4.30 a) by ρ , integrating the resulting expression over $0 < \rho < R$, and then using the divergence theorem. In passing to the limit $R \rightarrow \infty$, we note that since $v_2 = o(\rho^2 \log \rho)$ as $\rho \rightarrow \infty$ from (4.30 b), there is no contribution from the flux of $\Delta_\rho v_2$ across the big circle $\rho = R$. In this way, we obtain that

$$\lambda_1 = 8\lambda_0 \int_0^\infty \frac{v_1}{v_0^3} \rho d\rho, \quad (4.38)$$

where $v_0 = 2\rho^2 + 1$ and v_1 is given in (4.35). This expression can be evaluated explicitly upon integrating it by parts, and then using (4.33) for $v_{1\rho}$. In this way, we obtain

$$\begin{aligned} \lambda_1 &= \lambda_0 \int_0^\infty \left[\frac{1}{(1+2\rho^2)^2} \right] v_{1\rho} d\rho = 2\lambda_0 \log 2 \int_0^\infty \frac{\rho}{(1+2\rho^2)^2} d\rho - \lambda_0 \int_0^\infty \frac{\log(1+2\rho^2)}{\rho(1+2\rho^2)} d\rho, \\ &= \frac{\lambda_0}{2} \log 2 - \frac{\lambda_0}{2} \int_0^\infty \frac{\log(1+u)}{u(1+u)} du = \frac{\lambda_0}{2} \left(\log 2 - \frac{\pi^2}{6} \right) \approx -15.229. \end{aligned}$$

In the final step, the result $\int_0^\infty \log(1+u)/(u+u^2) du = \int_0^1 \log y/(y-1) dy = \pi^2/6$ has been used.

In terms of the known values of χ_1 , λ_0 , and λ_1 , we can obtain c_2 from (4.29 c). However, the expression for χ_2 in (4.29 c) gives only one equation for the two further unknowns c_1 and d_2 .

The solution v_2 of (4.30) is uniquely defined, and so provides the far-field behaviour

$$v_2 = -\frac{\lambda_0}{48} \log^3 \rho - \left(\frac{\lambda_1}{32} + \frac{\lambda_0}{32} \right) \log^2 \rho + \chi_3 \log \rho + \chi_4 + o(1), \quad \text{as } \rho \rightarrow \infty,$$

for some constants χ_3 and χ_4 determined in terms of the solution. Upon comparing this behaviour with (4.30 b) we get two equations

$$\chi_3 = d_2 - \frac{\lambda_2}{16} - \frac{\lambda_1}{32} - \frac{3\lambda_0}{64}, \quad \chi_4 = d_1 - e_2 - \frac{\lambda_2}{32} - \frac{3\lambda_1}{128} - \frac{13\lambda_0}{384}.$$

Therefore, d_2 is fixed in terms of λ_2 , which then determines c_1 from (4.29 c) for χ_2 . The equation for χ_4 gives one equation for d_1 and e_2 in terms of λ_2 . Similarly, we can continue this process to higher order to determine a further equation for d_1 and e_2 . We summarize the preceding calculation as follows:

Principal Result 4.1: *In the limit $\varepsilon \equiv u(0) + 1 \rightarrow 0^+$, the limiting asymptotic behaviour of the maximal radially symmetric solution branch of (4.1), away from a boundary layer region near $r = 0$, is given by*

$$u = u_0 + \frac{\varepsilon}{\sigma} \log \sigma u_{1/2} + \frac{\varepsilon}{\sigma} u_1 + \varepsilon \log \sigma u_{3/2} + \varepsilon u_2 + \mathcal{O}(\varepsilon \sigma \log \sigma), \quad \lambda = \frac{\varepsilon}{\sigma} [\lambda_0 + \sigma \lambda_1 + \mathcal{O}(\sigma^2)], \quad (4.39 a)$$

where $\sigma = -1/\log \gamma$ and the boundary layer width γ is determined in terms of ε by $-\gamma^2 \log \gamma = \varepsilon$. In (4.39 a),

$$u_0 = -1 + r^2 - 2r^2 \log r, \quad u_{1/2} = \frac{\lambda_0}{16} (1 - r^2 + 2r^2 \log r), \quad u_{3/2} = \frac{\lambda_1}{16} (1 - r^2 + 2r^2 \log r), \quad (4.39 b)$$

while u_1 and u_2 are the unique solutions of

$$\Delta^2 u_1 = -\frac{\lambda_0}{(1+u_0)^2}, \quad 0 < r < 1; \quad u_1(1) = u_{1r}(1) = 0, \quad (4.39 c)$$

$$u_1 = \frac{\lambda_0}{16} \log(-\log r) + \frac{\lambda_0}{16} + \mathcal{O}(\log^{-1} r), \quad r \rightarrow 0, \quad (4.39 d)$$

$$\Delta^2 u_2 = -\frac{\lambda_1}{(1+u_0)^2}, \quad 0 < r < 1; \quad u_2(1) = u_{2r}(1) = 0, \quad (4.39 e)$$

$$u_2 = \frac{\lambda_1}{16} \log(-\log r) + \frac{1}{16} (\lambda_0 + \lambda_1) - \log 2 + \frac{\lambda_0}{16} \log r + \mathcal{O}(\log^{-1} r), \quad r \rightarrow 0. \quad (4.39 f)$$

Finally, λ_0 and λ_1 are given by

$$\lambda_0 = 32, \quad \lambda_1 = \frac{\lambda_0}{2} \left(\log 2 - \frac{\pi^2}{6} \right). \quad (4.39 g)$$

In Fig. 10 we show a favourable comparison between the two-term asymptotic result for λ given in (4.39 a) and the corresponding full numerical result computed from (4.1).

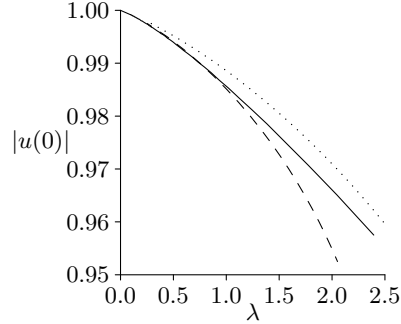


FIGURE 10. The one-term (dotted curve) and two-term (dashed curve) asymptotic results for $|u(0)| = 1 - \epsilon$ versus λ from (4.39 a) of Principal Result 4.1 are compared against the full numerical result (solid curve).

A very similar asymptotic analysis can be done for the mixed biharmonic problem (4.2). The main difference, as compared to the pure biharmonic case, is that now the leading-order outer solution u_0 satisfies

$$-\delta \Delta^2 u_0 + \Delta u_0 = 0, \quad 0 < r < 1; \quad u_0(1) = u_{0r}(1) = 0, \quad (4.40 a)$$

subject to the local behaviour

$$u_0 = -1 + \alpha r^2 \log r + \varphi r^2 + o(r^2), \quad \text{as } r \rightarrow 0, \quad (4.40 b)$$

for some α and φ , which depend on δ . The general solution of (4.40 a) is

$$u_0 = \mathcal{A} + \mathcal{B} \log r + \mathcal{C} K_0(\eta r) + \mathcal{D} I_0(\eta r), \quad \eta \equiv 1/\sqrt{\delta}, \quad (4.41)$$

where $K_0(z)$ and $I_0(z)$ are the usual modified Bessel functions. By satisfying the boundary conditions in (4.40 a), together with imposing the local behaviour (4.40 b) via the point constraints $u_0(0) = -1$ and $u_{0r}(0) = 0$, we obtain

$$\mathcal{A} = [I_0(\eta) (1 + \eta K_0'(\eta)) - \eta I_0'(\eta) K_0(\eta)] \mathcal{G}(\eta), \quad \mathcal{B} = \mathcal{C} = \eta I_0'(\eta) \mathcal{G}(\eta), \quad \mathcal{D} = -[1 + \eta K_0'(\eta)] \mathcal{G}(\eta), \quad (4.42 a)$$

where $\mathcal{G}(\eta)$ is defined by

$$\mathcal{G}(\eta) \equiv [\eta I_0'(\eta) (K_0(\eta) + \log(\eta/2) + \gamma_e) + (1 + \eta K_0'(\eta)) (1 - I_0(\eta))]^{-1}. \quad (4.42 b)$$

Here $\gamma_e \sim 0.5772$ is Euler's constant. By using (4.40 b) and (4.42), we can then explicitly calculate the functions $\alpha(\eta)$ and $\varphi(\eta)$ in (4.40 b) as

$$\alpha = -\left(\frac{\eta^3}{4}\right) I_0'(\eta) \mathcal{G}(\eta), \quad \varphi = -\frac{\eta^2}{4} [\eta I_0'(\eta) (\log(\eta/2) + \gamma_e - 1) + (1 + \eta K_0'(\eta))] \mathcal{G}(\eta). \quad (4.43)$$

In deriving (4.43) and (4.42), we have used the well-known small argument expansions $I_0(z) \sim 1 + z^2/4$ and $K_0(z) \sim -[\log(z/2) + \gamma_e] I_0(z) + z^2/4$ as $z \rightarrow 0$.

This explicit solution for α and φ has two key properties. Firstly, the limit $\delta \rightarrow \infty$, or equivalently $\eta \rightarrow 0$, corresponds to the pure biharmonic case. In this limit, we use the asymptotic behaviour of K_0 and I_0 to calculate

from (4.42 b) that $\mathcal{G} \sim 16/\eta^4$ as $\eta \rightarrow 0$. Upon using this result in (4.43), we can readily verify that $\alpha \rightarrow -2$ and $\varphi \rightarrow 1$ as $\eta \rightarrow 0$ ($\delta \rightarrow \infty$), in agreement with the pure biharmonic case result (4.5). Our second remark pertains to the sign of $\alpha(\eta)$. The asymptotic analysis leading to Principal Result 4.2 below requires that $\alpha < 0$ for all $\eta > 0$. This is readily verified numerically from the explicit formula for $\alpha(\eta)$ given in (4.43) (see Fig. 11(a) below). The main result characterizing the limiting form for the bifurcation diagram of (4.2) is as follows.

Principal Result 4.2: *In the limit $\varepsilon \equiv u(0) + 1 \rightarrow 0^+$, the limiting asymptotic behaviour of the maximal radially symmetric solution branch of (4.2), away from a boundary layer region near $r = 0$, is given by*

$$u = u_0 + \frac{\varepsilon}{\sigma} \log \sigma u_{1/2} + \frac{\varepsilon}{\sigma} u_1 + \varepsilon \log \sigma u_{3/2} + \varepsilon u_2 + \mathcal{O}(\varepsilon \sigma \log \sigma), \quad \lambda = \frac{\delta \varepsilon}{\sigma} [\lambda_0 + \sigma \lambda_1 + \mathcal{O}(\sigma^2)], \quad (4.44 a)$$

where $\sigma = -1/\log \gamma$ and the boundary layer width γ is determined in terms of ε by $-\gamma^2 \log \gamma = \varepsilon$. In (4.44 a),

$$u_0 = \mathcal{A} + \mathcal{B} \log r + \mathcal{C} K_0(\eta r) + \mathcal{D} I_0(\eta r), \quad u_{1/2} = -\frac{\lambda_0}{4\alpha^2} u_0, \quad u_{3/2} = -\frac{\lambda_1}{4\alpha^2} u_0, \quad (4.44 b)$$

where \mathcal{A} , \mathcal{B} , \mathcal{C} , and \mathcal{D} are defined in (4.42). Moreover, u_1 and u_2 are the unique solutions of

$$\Delta^2 u_1 - \eta^2 \Delta u_1 = -\frac{\lambda_0}{(1+u_0)^2}, \quad 0 < r < 1; \quad u_1(1) = u_{1r}(1) = 0, \quad (4.44 c)$$

$$u_1 \sim \frac{\lambda_0}{4\alpha^2} \log(-\log r) + \frac{\lambda_0}{4\alpha^2} + \mathcal{O}(\log^{-1} r), \quad \text{as } r \rightarrow 0, \quad (4.44 d)$$

$$\Delta^2 u_2 - \eta^2 \Delta u_2 = -\frac{\lambda_1}{(1+u_0)^2}, \quad 0 < r < 1; \quad u_2(1) = u_{2r}(1) = 0, \quad (4.44 e)$$

$$u_2 \sim \frac{\lambda_0}{4\alpha^2} \log(-\log r) + \frac{\lambda_0}{4\alpha^2} \log r + \frac{\lambda_0}{2\alpha^2} \left(1 + \frac{\varphi}{\alpha}\right) + \frac{\lambda_1}{4\alpha^2} - \log(-\alpha) + \mathcal{O}(\log^{-1} r), \quad \text{as } r \rightarrow 0, \quad (4.44 f)$$

where $\eta \equiv \delta^{-1/2}$. Finally, λ_0 and λ_1 are given by

$$\lambda_0 = 8\alpha^2, \quad \lambda_1 = -\frac{\lambda_0}{2} \left[\frac{\pi^2}{6} - \log(-\alpha) + \left(1 + \frac{2\varphi}{\alpha}\right) \right]. \quad (4.44 g)$$

Since $\alpha < 0$ for all $\eta > 0$, the formulae in Principal Result 4.2 are well-defined. In Fig. 11(a) we plot the coefficients α and φ versus δ , defined in (4.43), while in Fig. 11(b) we plot the coefficients $\delta\lambda_0$ and $\delta\lambda_1$ in the expansion (4.44 a) versus δ , where λ_0 and λ_1 are defined in (4.44 g). For various fixed values of δ , in Fig. 12 we show a very favourable comparison between our asymptotic result for the limiting behaviour of the maximal solution branch and the corresponding full numerical result computed from (4.2).

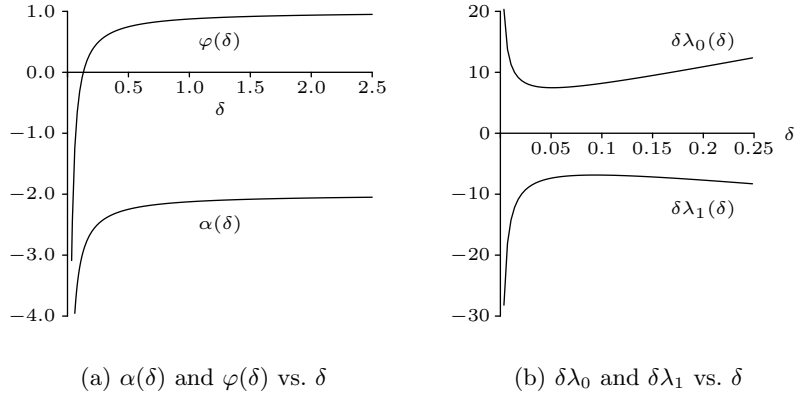


FIGURE 11. Left figure: $\alpha(\delta)$ and $\varphi(\delta)$, defined in (4.43), are plotted for $0 < \delta < 2.5$. Notice that $(\alpha, \varphi) \rightarrow (-2, 1)$ as $\delta \rightarrow \infty$ in agreement with the pure biharmonic case. Right figure: $\delta\lambda_0$ and $\delta\lambda_1$ versus δ , where λ_0 and λ_1 are defined in (4.44 g).

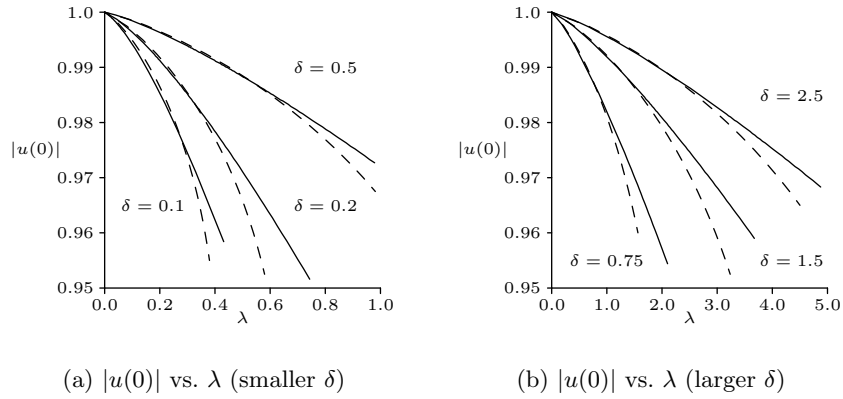


FIGURE 12. The two-term asymptotic results (dashed curves) for $|u(0)| = 1 - \varepsilon$ versus λ from (4.44 a) of Principal Result 4.2 are compared with full numerical results (solid curves). Left figure: smaller values of δ . Right figure: larger values of δ .

5 The Annulus Problem in the Unit Disk

In this section we construct the limiting asymptotic behaviour of the maximal solution branch for the annular MEMS problem (1.4) in a concentric annular domain in \mathbb{R}^2 formulated as

$$\Delta u = \frac{\lambda}{(1+u)^2}, \quad \delta \leq r \leq 1; \quad u(\delta) = u(1) = 0, \quad (5.1)$$

with $0 < \delta < 1$ and $\delta = \mathcal{O}(1)$. We seek a solution of (5.1) for which $\lambda \rightarrow 0$ as $u(r_\varepsilon) + 1 \equiv \varepsilon \rightarrow 0$, where r_ε is a free-boundary point to be determined. This problem, which is analyzed by formal asymptotic methods, is related to the problem studied rigorously in [9].

In the outer region, defined away from r_ε , we try an expansion for the outer solution u and for λ in the form

$$u = u_0 + \nu u_1 + \dots, \quad \lambda = \nu(\lambda_0 + \mu\lambda_1 + \dots), \quad (5.2)$$

where $\nu \ll 1$ and $\mu \ll 1$ are gauge functions to be determined. As shown below, this expansion must be adjusted by

inserting a certain switchback term in the outer expansion. From (5.2) and (5.1), we obtain that u_0 and u_1 satisfy

$$\Delta u_0 = 0, \quad \delta < r < r_\varepsilon, \quad r_\varepsilon < r < 1; \quad u_0(\delta) = u_0(1) = 0, \quad (5.3 a)$$

$$\Delta u_1 = \frac{\lambda_0}{(1+u_0)^2}, \quad \delta < r < r_\varepsilon, \quad r_\varepsilon < r < 1; \quad u_1(\delta) = u_1(1) = 0. \quad (5.3 b)$$

Upon imposing the point constraint that $u_0(r_\varepsilon) = -1$, we obtain from (5.3 a) that u_0 satisfies

$$u_0 = \begin{cases} -\log(r/\delta)/\log(r_\varepsilon/\delta), & \delta < r < r_\varepsilon \\ -\log r/\log r_\varepsilon, & r_\varepsilon < r < 1, \end{cases} \quad (5.4)$$

and is not differentiable at r_ε . Then, since $u_0 \sim -1 + u_{0r}(r_\varepsilon^\pm)(r - r_\varepsilon)$ as $r \rightarrow r_\varepsilon^\pm$, we obtain from (5.3 b) that u_1 satisfies $\Delta u_1 = \lambda_0(r - r_\varepsilon)^{-2}/[u_{0r}(r_\varepsilon^\pm)]^2$ as $r \rightarrow r_\varepsilon$. Therefore, u_1 must have the near-field behaviour

$$u_1 \sim -\frac{\lambda_0}{[u_{0r}(r_\varepsilon^\pm)]^2} \log|r - r_\varepsilon| + a_1 + o(1), \quad \text{as } r \rightarrow r_\varepsilon^\pm, \quad (5.5)$$

where a_1 is a constant associated with the homogeneous solution to (5.3 b). From (5.2), (5.4), and (5.5), we obtain that the outer expansion has the limiting behaviour

$$u \sim -1 + u_{0r}(r_\varepsilon^\pm)(r - r_\varepsilon) + \frac{u_{0rr}(r_\varepsilon^\pm)}{2}(r - r_\varepsilon)^2 + \nu \left[-\frac{\lambda_0}{[u_{0r}(r_\varepsilon^\pm)]^2} \log|r - r_\varepsilon| + a_1 + o(1) \right], \quad \text{as } r \rightarrow r_\varepsilon^\pm. \quad (5.6)$$

In the inner region near r_ε , we introduce the inner variables v and ρ by

$$u = -1 + \varepsilon v(\rho), \quad \rho = (r - r_\varepsilon)/\gamma,$$

where $\gamma \ll 1$ is the internal layer width to be determined. The leading-order term in the local behaviour (5.6) of the outer expansion gives $u \sim -1 + \gamma u_{0r}(r_\varepsilon^\pm)\rho$, which must match with the inner expansion $u = -1 + \varepsilon v$. Therefore, we must take $\gamma = \varepsilon$, and to leading order we must impose that $v \sim u_{0r}(r_\varepsilon^\pm)\rho$ as $\rho \rightarrow \pm\infty$. With $\lambda \sim \nu[\lambda_0 + \mu\lambda_1 + \dots]$ and $\gamma = \varepsilon$, the inner problem for $v(\rho)$ from (5.1) is

$$v'' + \frac{\varepsilon v'}{r_\varepsilon + \varepsilon\rho} = \frac{\nu}{\varepsilon} \frac{[\lambda_0 + \mu\lambda_1 + \dots]}{v^2}, \quad (5.7)$$

which suggests that $\nu = \varepsilon$. The scale of μ relative to ε is at this stage unknown. Therefore, to leading order, we set $r_\varepsilon \sim r_0 + o(1)$ and $v \sim v_0$ to obtain that

$$v_0'' = \frac{\lambda_0}{v_0^2}, \quad -\infty < \rho < \infty; \quad v_0(0) = 1, \quad v_0'(0) = 0; \quad v_0 \sim u_{0r}(r_0^\pm)\rho, \quad \text{as } \rho \rightarrow \pm\infty. \quad (5.8)$$

The condition $v_0(0) = 1$ and $v_0'(0) = 0$, with $v_0''(0) > 0$, is a necessary and sufficient condition for u to have its minimum value of $-1 + \varepsilon$ at $r_\varepsilon = r_0 + o(1)$. From (5.8) we conclude that v_0 is even in ρ , and consequently r_0 satisfies $u_{0r}(r_0^+) = -u_{0r}(r_0^-)$. From (5.4), this equation for r_0 reduces to $\log r_0 = -\log(r_0/\delta)$, which yields $r_0 = \sqrt{\delta}$. To determine λ_0 , we first multiply the equation (5.8) for v_0 by v_0' , and then integrate it from $0 < y < \infty$ to get

$$\frac{1}{2} [v_0'(\infty)]^2 = \lambda_0 \int_0^\infty \frac{v_0'}{v_0^2} dy = \lambda_0 \int_1^\infty \frac{dv_0}{v_0^2} = \lambda_0 \left(-\frac{1}{v_0} \right) \Big|_1^\infty = \lambda_0. \quad (5.9)$$

Then, by using $v_0'(\infty) = u_{0r}(r_0^+) = [r_0 \log r_0]^{-2}$ and $r_0 = \sqrt{\delta}$, we conclude from (5.9) that $\lambda_0 = 2[\delta(\log \delta)^2]^{-1}$.

To construct a higher-order expansion for λ , the free boundary location r_ε , and the inner and outer expansions for (5.1), we first must calculate further terms in the far-field behaviour of v_0 as $\rho \rightarrow \pm\infty$. To do so, we integrate the first integral of (5.8) for v_0 to obtain an implicitly-defined exact solution of (5.8), given by

$$\sqrt{v_0(v_0 - 1)} + \log(\sqrt{v_0} + \sqrt{v_0 - 1}) = \sqrt{2\lambda_0}\rho, \quad \text{for } \rho \geq 0. \quad (5.10)$$

Since $\sqrt{2\lambda_0} = u_{0r}(r_0^+) = -u_{0r}(r_0^-)$, and $v_0(\rho) = v_0(-\rho)$, the far-field far-field behaviour for v_0 as $\rho \rightarrow \pm\infty$, obtained from (5.10), is

$$v_0 \sim \pm u_0(r_0^+) \rho - \frac{\lambda_0}{[u_{0r}(r_0^+)]^2} \log \rho + \chi, \quad \text{as } \rho \rightarrow \pm\infty; \quad \chi \equiv \frac{1}{2} - \log 2 - \frac{1}{4} \log(2\lambda_0). \quad (5.11)$$

Next, we substitute $r - r_\varepsilon = \varepsilon \rho$ into the local behaviour of the outer expansion (5.6) to obtain

$$u \sim -1 - \varepsilon \log \varepsilon \frac{\lambda_0}{[u_{0r}(r_\varepsilon^\pm)]^2} + \varepsilon \left[u_{0r}(r_\varepsilon^\pm) \rho - \frac{\lambda_0}{[u_{0r}(r_\varepsilon^\pm)]^2} \log \rho + a_1 \right] + \frac{\varepsilon^2}{2} u_{0rr}(r_\varepsilon^\pm) \rho^2. \quad \text{as } r \rightarrow r_\varepsilon^\pm. \quad (5.12)$$

The constant $\mathcal{O}(\varepsilon \log \varepsilon)$ term in (5.12) cannot be accounted for by the inner expansion. Thus, we must adjust the outer expansion for u_0 in (5.2) by inserting a switchback term. The modified outer expansion, in place of (5.2), is

$$u = u_0 + (-\varepsilon \log \varepsilon) u_{1/2} + \varepsilon u_1 + \dots; \quad \lambda = \varepsilon (\lambda_0 + \mu \lambda_1 + \dots). \quad (5.13)$$

Upon substituting (5.13) into (5.1), we obtain that $u_{1/2}(r)$ satisfies

$$\Delta u_{1/2} = 0, \quad \delta < r < r_\varepsilon, \quad r_\varepsilon < r < 1; \quad u_{1/2}(\delta) = u_{1/2}(1) = 0. \quad (5.14)$$

By enforcing the point constraint $u_{1/2}(r_\varepsilon) = -\lambda_0 / [u_{0r}(r_\varepsilon^\pm)]^2$, we can eliminate the constant term of order $\mathcal{O}(\varepsilon \log \varepsilon)$ in (5.12). In this way, the solution to (5.14) can be written in terms of u_0 as

$$u_{1/2}(r) = \frac{\lambda_0}{[u_{0r}(r_\varepsilon^\pm)]^2} u_0(r). \quad (5.15)$$

In addition, we must seek a higher-order expansion for the free-boundary point as

$$r_\varepsilon = r_0 + \sigma r_1 + \dots, \quad (5.16)$$

where $r_0 = \sqrt{\delta}$ and the gauge function $\sigma \ll 1$ is to be found.

To determine the matching condition between the inner expansion $u = -1 + \varepsilon(v_0 + \mu v_1 + \dots)$ and the modified outer expansion (5.13), we add the local behaviour of $(-\varepsilon \log \varepsilon) u_{1/2}$ as $r \rightarrow r_\varepsilon$ to (5.12) and use (5.16) for r_ε . In addition, we use the far-field behaviour (5.11) for v_0 . The matching condition, written in terms of ρ , is

$$\begin{aligned} -1 + \varepsilon \left[u_{0r}(r_0^\pm) \rho - \frac{\lambda_0}{[u_{0r}(r_0^\pm)]^2} \log \rho + a_1 \right] + \varepsilon \sigma r_1 u_{0rr}(r_0^\pm) \rho + (-\varepsilon^2 \log \varepsilon) u_{1/2r}(r_0^\pm) \rho + \mathcal{O}(\varepsilon^2) \\ \sim -1 + \varepsilon \left[u_{0r}(r_0^\pm) \rho - \frac{\lambda_0}{[u_{0r}(r_0^\pm)]^2} \log \rho + \chi \right] + \varepsilon \mu v_1 + \dots. \end{aligned} \quad (5.17)$$

This matching condition determines μ , σ , and a_1 , as

$$\mu = -\varepsilon \log \varepsilon, \quad \sigma = -\varepsilon \log \varepsilon, \quad a_1 = \chi = \frac{1}{2} - \log 2 - \frac{1}{4} \log(2\lambda_0), \quad (5.18)$$

Since $\mu = -\varepsilon \log \varepsilon \gg \mathcal{O}(\varepsilon)$, we conclude from (5.7) and (5.17) that the inner correction v_1 satisfies

$$\mathcal{L}v_1 \equiv v_1'' + \frac{2\lambda_0}{v_0^3} v_1 = \frac{\lambda_1}{v_0^2}, \quad -\infty < \rho < \infty, \quad (5.19 a)$$

$$v_1(0) = 0; \quad v_1 \sim [u_{0rr}(r_0^\pm) r_1 + u_{1/2r}(r_0^\pm)] \rho, \quad \text{as } \rho \rightarrow \pm\infty. \quad (5.19 b)$$

Since $u_{0rr}(r_0^\pm) = \mp u_{0r}(r_0^+) / r_0$ from (5.3 a), and $u_{1/2r}(r_0^\pm) = \pm \lambda_0 / [u_{0r}(r_0^+)]$, as obtained from the explicit solution (5.15), the far-field condition (5.19 b) becomes

$$v_1 \sim \pm A \rho, \quad \text{as } \rho \rightarrow \pm\infty; \quad A \equiv -\frac{r_1}{r_0} u_{0r}(r_0^+) + \frac{\lambda_0}{u_{0r}(r_0^+)}. \quad (5.19 c)$$

Since v_0 is an even function, the general solution to (5.19 a) must be the sum of an even and odd function. The condition $v_1(0) = 0$ enforces that v_1 is odd, and consequently we must have $A = 0$ in (5.19 c). Since $\lambda_0 = [u_{0r}(r_0^+)]^2/2$, the condition that $A = 0$ determines r_1 as $r_1 = r_0/2$. Finally, we determine λ_1 from a solvability condition. We multiply (5.19 a) by v_0' , and use $\mathcal{L}v_0' = 0$, to obtain

$$\int_0^\infty v_0' \mathcal{L}v_1 d\rho = \lambda_1 \int_0^\infty \frac{v_0'}{v_0^2} d\rho = Av_0'(\infty). \quad (5.20)$$

However, since $A = 0$, we get $\lambda_1 = 0$. We summarize the preceding calculation as follows:

Principal Result 5.1: *In the limit $\varepsilon \equiv u(r_\varepsilon) + 1 \rightarrow 0^+$ for some free-boundary point r_ε , the limiting asymptotic behaviour of the maximal radially symmetric solution branch of (5.1), away from the internal layer region near $r = r_\varepsilon$, is*

$$u \sim u_0(r) + (-\varepsilon \log \varepsilon) \frac{\lambda_0}{[u_{0r}(r_0)]^2} u_0(r) + \varepsilon u_1(r) + \dots. \quad (5.21 a)$$

Here, u_0 is given in (5.4) and u_1 satisfies (5.3 b) subject to

$$u_1 \sim -\frac{\lambda_0}{[u_{0r}(r_0)]^2} \log |r - r_0| + \chi + o(1), \quad \text{as } r \rightarrow r_0, \quad (5.21 b)$$

where χ is defined in (5.11). Finally, λ and the free-boundary point r_ε are given for $\varepsilon \rightarrow 0$ by

$$\lambda \sim \frac{2\varepsilon}{\delta [\log \delta]^2} + o(\varepsilon^2 \log \varepsilon), \quad r_\varepsilon \sim \sqrt{\delta} \left[1 + \frac{(-\varepsilon \log \varepsilon)}{2} + \dots \right]. \quad (5.21 c)$$

In Fig. 13 we compare the asymptotic prediction for λ given in (5.21 c) with the corresponding full numerical result computed from (5.1). Notice that, owing to the small error term in (5.21 c) for λ , the asymptotic result for λ accurately predicts the full numerical result for λ even when ε is not too small.

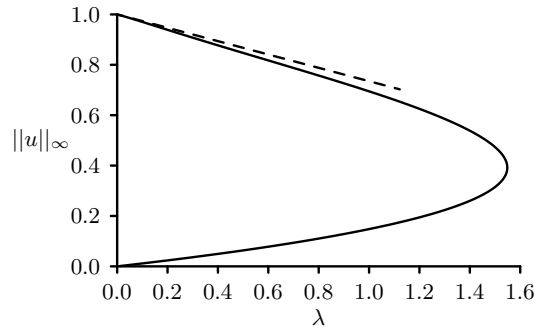


FIGURE 13. Comparison of numerical solution for $\|u\|_\infty$ versus λ (heavy solid curve) computed from the annulus problem (1.4) in $\delta < r < 1$ for $\delta = 0.1$ with the limiting asymptotic approximation (5.21 c) (dashed curve) valid for $\lambda \rightarrow 0$.

6 Discussion

In this paper we have developed a systematic asymptotic approach for constructing the limiting asymptotic behaviour of the infinite fold-point structure for (1.3), and we have calculated the asymptotic behaviour as $\lambda \rightarrow 0$ of the maximal solution branch for the biharmonic MEMS problem (1.1) and the annulus problem (1.4). The common feature in the analysis has been the use of a small parameter $\varepsilon \equiv 1 - \|u\|_\infty$ that renders the nonlinearity $(1 + u)^{-2}$ nearly singular as $\varepsilon \rightarrow 0$ in some narrow spatial zone of concentration. The results from the asymptotic analysis have been shown to

compare very favourably with full numerical results. Our formal asymptotic analysis is one of the first explicit studies of concentration phenomena for a biharmonic problem nonlinear eigenvalue problem. We conclude by remarking on three directions that warrant further study.

Firstly, it would be interesting to provide a quantitative asymptotic theory describing the precise mechanism for the destruction of the infinite fold-point structure for (1.2) when (1.2) is perturbed for $0 < \delta \ll 1$ to either the biharmonic problem (1.1) or the annulus problem (1.4). In particular, can one predict analytically the number of fold points for each of these perturbed problems as $\delta \rightarrow 0$?

Secondly, it would be interesting to extend the analysis in §4 for the biharmonic nonlinear eigenvalue problem in the unit disk to an arbitrary two-dimensional domain. In particular, can one construct the limiting asymptotic form of the maximal solution branch in terms of the biharmonic Green's function for solutions exhibiting either single or multiple concentration points? Solutions with concentration phenomena have been well-studied for quasilinear elliptic problems in arbitrary two-dimensional domains, but there are only a few results to date for corresponding nonlinear biharmonic problems. Work in this direction is given in [17].

Finally, it would be interesting to give a precise description of the asymptotic behaviour of the bifurcation curve of radially symmetric solutions to the following so-called fringing-field problem in the unit disk in \mathbb{R}^2 :

$$\Delta u = \frac{\lambda}{(1+u)^2} (1 + \delta |\nabla u|^2), \quad x \in \Omega; \quad u = 0, \quad x \in \partial\Omega. \quad (6.1)$$

This model with $\delta > 0$ was derived in [25] upon including the effect of a fringing electrostatic field of a MEMS capacitor that has a finite spatial extent. It would be interesting to give a detailed quantitative analysis showing both how the infinite-fold point structure of the unperturbed problem (1.2) gets destroyed when $0 < \delta \ll 1$, and deriving the limiting behavior of the maximal solution branch for (6.1) corresponding to $\lambda \rightarrow 0$ as $\varepsilon = u(0) + 1 \rightarrow 0^+$ with $\delta > 0$ fixed. The destruction of the infinite fold-point structure for (6.1) when $\delta > 0$ was studied numerically using a dynamical systems approach in [25], and some rigorous results were obtained in [28].

Acknowledgements

A. L. was supported by an NSERC (Canada) graduate fellowship, and M. J. W. was supported by NSERC (Canada). We are grateful to Prof. J. Wei for several helpful discussions.

References

- [1] D. Cassani, J. Marcos do Ó, N. Ghoussoub, *On a Fourth Order Elliptic Problem with a Singular Nonlinearity*, J. Advanced Nonlinear Studies, **9**, (2009), pp. 177–197.
- [2] C. Cowan, P. Esposito, N. Ghoussoub, A. Moradifam, *The Critical Dimension for a Fourth Order Elliptic Problem with Singular Nonlinearity*, Arch. Rational Mech. Anal., to appear, (2009), (19 pages).
- [3] C. Cowan, N. Ghoussoub, *Estimates on Pull-In Distances in MEMS Models and Other Nonlinear Eigenvalue Problems*, submitted, (2009), (17 pages)
- [4] P. Esposito, N. Ghoussoub, *Uniqueness of Solutions for an Elliptic Equation Modeling MEMS*, Methods Appl. Anal., **15**, No. 3, (2008), pp. 341–353.
- [5] P. Esposito, N. Ghoussoub, Y. Guo, *Compactness Along the Branch of Semi-Stable and Unstable Solutions for an Elliptic Equation with a Singular Nonlinearity*, Comm. Pure Appl. Math. **60**, No. 12, (2007), pp. 1731–1768.
- [6] P. Esposito, N. Ghoussoub, Y. Guo, *Mathematical Analysis of Partial Differential Equations Modeling Electrostatic MEMS*, Courant Lecture Notes, in press, (2009), 332 pp.
- [7] P. Feng, Z. Zhou, *Multiplicity and Symmetry Breaking for Positive Radial Solutions of Semilinear Elliptic Equations Modeling MEMS on Annular Domains*, Electr. J. Diff. Equat., No. 146, (2005), 14 pp. (electronic)

- [8] N. Ghoussoub, Y. Guo, *On the Partial Differential Equations of Electrostatic MEMS Devices: Stationary Case*, SIAM J. Math. Anal., **38**, No. 5, (2006/07), pp. 1423–1449.
- [9] M. Grossi, *Asymptotic Behaviour of the Kazdan-Warner Solution in the Annulus*, J. Differential Equations, **223**, No. 1, (2006), pp. 96–111.
- [10] Y. Guo, Z. Pan, M. J. Ward, *Touchdown and Pull-In Voltage Behaviour of a MEMS Device with Varying Dielectric Properties*, SIAM J. Appl. Math., **66**, No. 1, (2005), pp. 309–338.
- [11] Z. Guo, J. Wei, *Symmetry of Nonnegative Solutions of a Semilinear Elliptic Equation with Singular Nonlinearity*, Proc. Roy. Soc. Edinburgh Sect. A, **137**, No. 5, (2007), pp. 963–994.
- [12] Z. Guo, J. Wei, *Infinitely Many Turning Points for an Elliptic Problem with a Singular Nonlinearity*, Journ. London Math. Society, **78**, (2008), pp. 21–35.
- [13] Z. Guo, J. Wei, *Asymptotic Behaviour of Touchdown Solutions and Global Bifurcations for an Elliptic Problem with a Singular Nonlinearity*, Comm. Pure. Appl. Analysis, **7**, No. 4, (2008), pp. 765–787.
- [14] Z. Guo, J. Wei, *Entire Solutions and Global Bifurcations for a Biharmonic Equation with Singular Nonlinearity in \mathbb{R}^3* , Advances Diff. Equations, **13**, (2008), No. 7-8, pp. 743–780.
- [15] Z. Guo, J. Wei, *On a Fourth Order Nonlinear Elliptic Equation with Negative Exponent*, SIAM J. Math. Anal., **40**, No. 5, (2009), pp. 2034–2054.
- [16] D. Joseph, T. Lundgren *Quasilinear Dirichlet Problems Driven by Positive Sources*, Arch. Rational Mech. Anal. **49** (1972/73), pp. 241–269.
- [17] M. C. Kropinski, A. Lindsay, M. J. Ward, *Concentration Phenomena for Some Fourth-Order Singularly Perturbed Linear and Nonlinear Eigenvalue Problems in Two-Dimensional Domains*, in preparation, (2010).
- [18] P. Lagerstrom, *Matched Asymptotic Expansions: Ideas and Techniques*, Applied Mathematical Sciences, **76**, Springer-Verlag, New York, (1988).
- [19] P. Lagerstrom, D. Reinelt, *Note on Logarithmic Switchback Terms in Regular and Singular Perturbation Problems*, SIAM J. Appl. Math., **44**, No. 3, (1984), pp. 451–462.
- [20] F. H. Lin, Y. Yang, *Nonlinear Non-Local Elliptic Equation Modeling Electrostatic Actuation*, Proc. Roy. Soc. A, **463**. (2007), pp. 1323–1337.
- [21] A. Lindsay, M. J. Ward, *Asymptotics of Some Nonlinear Eigenvalue Problems for a MEMS Capacitor: Part I: Fold Point Asymptotics*, Methods Appl. Anal., **15**, No. 3, (2008), pp. 297–325.
- [22] J. A. Pelesko, D. H. Bernstein, *Modeling MEMS and NEMS*, Chapman Hall and CRC Press, (2002).
- [23] J. A. Pelesko, *Mathematical Modeling of Electrostatic MEMS with Tailored Dielectric Properties*, SIAM J. Appl. Math., **62**, No. 3, (2002), pp. 888–908.
- [24] J. A. Pelesko, D. Bernstein, J. McCuan, *Symmetry and Symmetry Breaking in Electrostatic MEMS*, Proceedings of MSM 2003, (2003), pp. 304–307.
- [25] J. A. Pelesko, T. A. Driscoll, *The Effect of the Small Aspect Ratio Approximation on Canonical Electrostatic MEMS Models*, J. Engrg. Math., **53**, No. 3-4, (2005), pp. 239–252.
- [26] N. Popovic, P. Szymolyan, *A Geometric Analysis of the Lagerstrom Model Problem*, J. Differential Equations, **199**, No. 2, (2004), pp. 290–325.
- [27] N. Popovic, P. Szymolyan, *Rigorous Asymptotic Expansions for Lagerstrom’s Model Equation - A Geometric Approach*, Nonlinear Anal., **59**, No. 4, (2004), pp. 531–565.
- [28] J. Wei, D. Ye, *On MEMS Equation with Fringing Field*, to appear, Proc. Amer. Math. Soc., (2010), (8 pages).